International Journal of Current Science Research and Review
ISSN: 2581-8341
Volume 09 Issue 08 August 2026
DOI: 10.47191/ijcsrr/V9-i8-44, Impact Factor: 8.048
IJCSRR @ 2026
www.ijcsrr.org

From Magnesium Feedstocks to Reactive MgO: A Critical Review of Production Routes, Reactivity Control, Industrial Scalability, and Environmental Trade-Offs

Antonio Clareti Pereira, PhD
PhD in Chemical Engineering
University of São Paulo (USP)
Belo Horizonte, Minas Gerais, Brazil
ORCID: https://orcid.org/0000-0001-8115-4279

ABSTRACT: Reactive magnesium oxide (r-MgO) is often treated as a single material class, yet its performance is governed by a chain of coupled decisions extending from magnesium source and precursor chemistry to heat and mass transfer, calcination severity, atmosphere, particle size, purification, and post-calcination aging. This structured critical narrative review reframes reactive MgO production as a process–structure–reactivity engineering problem rather than a catalog of synthesis methods. A fixed core evidence corpus of 103 publications from 2020 through August 2026 was coded by production route, evidence scale, reactivity endpoint, and environmental/economic dimension; three pre-2020 foundational sources were used only for terminology and mechanistic context and were excluded from corpus counts. The review compares mineral-derived, brucite-derived, dolomitic, seawater/brine, waste-derived, sulfate-derived, and specialty precursors; conventional, flash, fluidized-bed, steam-assisted, solar/electrified, precipitation, carbonation, electrochemical, and hybrid routes; and the analytical methods used to describe reactivity. No single metric—calcination temperature, BET surface area, hydration rate, or CO_2 uptake—defines reactive MgO across applications. Instead, reactivity emerges from the preservation or destruction of accessible mesoporosity, surface defects, dissolution sites, crystallite-scale disorder, and pore connectivity, provided that sufficient precursor conversion and chemical purity are achieved. Fast thermal routes can reduce sintering exposure, whereas brine and residue routes can decouple purity from the original mineralogy but introduce reagent demand, washing, mother-liquor management, and scale-up penalties. Environmental advantage is likewise route-specific: avoiding magnesite decarbonation can reduce process CO_2, but upstream alkalis, electricity, solids handling, and unrealized carbonation can reverse apparent benefits. The industrially optimum product is therefore not the MgO with the highest nominal reactivity, but the product whose application-specific reactivity window is achieved at acceptable purity, energy demand, carbon footprint, cost, throughput, and consistency. The review concludes with a research agenda centered on standardized reporting, direct route-to-route experiments, impurity-tolerance maps, continuous pilot validation, and integrated mass–energy–carbon–cost assessment.

KEYWORDS: calcination, industrial scale-up, reactive magnesia, magnesium oxide, seawater brine, process–structure–reactivity.

Highlights

- Reactivity is an engineered process outcome rather than a temperature-defined MgO class.
- Fast calcination can preserve reactive microstructure, but scale-up depends on heat and mass transfer control.
- Brine and waste routes can improve circularity and purity but may shift burdens to reagents, washing, and mother-liquor treatment.
- The preferred industrial route is the one that meets an application-specific reactivity window at minimum energy, carbon, cost, and complexity.

International Journal of Current Science Research and Review
ISSN: 2581-8341
Volume 09 Issue 08 August 2026
DOI: 10.47191/ijcsrr/V9-i8-44, Impact Factor: 8.048
IJCSRR @ 2026
www.ijcsrr.org

Graphical abstract

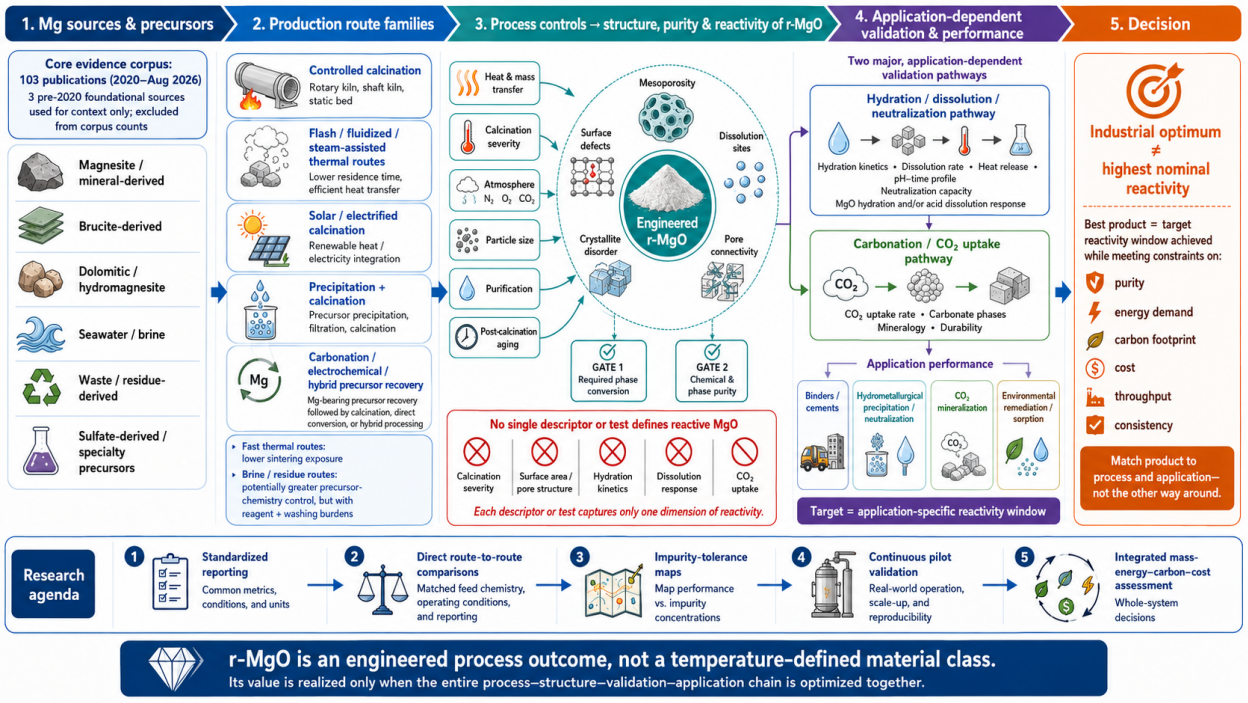

1. INTRODUCTION

1.1. Reactive MgO as a process-dependent material

Magnesium oxide spans an unusually broad spectrum of industrial functions: refractory and insulating service, cementitious and expansive binders, neutralization and precipitation, sorption, environmental remediation, catalysis, and carbon mineralization. The same nominal formula, MgO, can therefore describe products whose behavior in water or acid differs by orders of practical importance. Recent literature increasingly shows that the useful distinction is not simply between ‘MgO’ and ‘reactive MgO’, but between materials carrying different thermal, chemical, and morphological histories. Low-temperature decomposition, precursor morphology, porosity, defect density, accessible surface and impurity chemistry jointly govern dissolution, hydration and carbonation pathways (Bassioni et al., 2021; Bernard et al., 2023; Bracco et al., 2024; Gevaudan et al., 2026; Huang et al., 2020; Nobre et al., 2020; Pettauer et al., 2024; Wang et al., 2026).

This process dependence is especially important because conventional magnesia nomenclature—caustic-calcined or light-burned, hard-burned, dead-burned, and high-surface-area or nanostructured MgO—blurs the lines among processing history, performance, and market convention. Calcination temperature remains useful as an operating descriptor, but it is an incomplete classifier: the same peak temperature can yield different MgO when the heating rate, residence time, atmosphere, precursor chemistry, particle size, gas–solid contact, and cooling history differ. Studies of magnesite, brucite, hydromagnesite and light-burned MgO illustrate this non-uniqueness (Are et al., 2022; Chen et al., 2025; Hou et al., 2021; Hu et al., 2024; Huang et al., 2020; Li et al., 2025; Lim et al., 2022; Salomão et al., 2020; Smadi et al., 2023; Tan et al., 2025; Zhou et al., 2024; Zhou et al., 2026). The long-standing industrial distinction among caustic-calcined, hard-burned, and dead-burned magnesia also reflects this dependence on thermal history (Shand, 2006).

1.2. From conventional magnesia to engineered reactive MgO

For this review, reactive MgO is defined operationally rather than by a fixed temperature threshold. It is MgO engineered to provide a reproducible rate and extent of reaction in a specified environment, while satisfying required purity, particle characteristics and handling behavior. This definition deliberately separates ‘high reactivity’ from ‘high surface area’. Mesopores and defects can be decisive, but an extremely high BET value is not automatically useful if pores are inaccessible, dissolution is diffusion-limited,

International Journal of Current Science Research and Review
ISSN: 2581-8341
Volume 09 Issue 08 August 2026
DOI: 10.47191/ijcsrr/V9-i8-44, Impact Factor: 8.048
IJCSRR @ 2026
www.ijcsrr.org

impurities passivate the surface, or the material reacts too early during storage or formulation (Bracco et al., 2024; Li et al., 2020; Pettauer et al., 2024; Tang et al., 2025; Wang et al., 2026; Weber et al., 2025).

The engineering implication is that product design must begin from the application. Cobalt precipitation requires a different balance of dissolution and alkalinity delivery from magnesium phosphate cement, permeable reactive barriers, CO_2 mineralization, or specialty nanomaterials. The literature already contains examples in which MgO activity is evaluated through cobalt precipitation, heavy-metal removal, binder hydration, arsenic immobilization, and ambient carbonation; these studies demonstrate that performance is conditional on the reacting system rather than an intrinsic scalar property (Chen et al., 2026; Fedoročková et al., 2021; Gu et al., 2026; Lee et al., 2025; Liu, Li, Yu, et al., 2025; McQueen et al., 2020).

1.3. Why production route matters

The central hypothesis of this review is a causal chain: feedstock composition determines precursor chemistry and impurity burden; the precursor then experiences a thermal or chemical history that controls decomposition, nucleation, crystal growth, sintering and pore evolution; these structural features determine measurable reactivity; and measurable reactivity only becomes meaningful when translated into application performance. Direct mineral calcination and indirect precipitation routes therefore cannot be compared on peak temperature or purity alone. Their benefits and liabilities must be traced through the entire process chain (Ababneh et al., 2025; An et al., 2021; An et al., 2025; Chu et al., 2023; Dong et al., 2023; Ma et al., 2023; Ma et al., 2024; Romano et al., 2023; Ruan et al., 2021; Taheri & Larachi, 2025).

This framing also resolves an apparent contradiction in the literature. Advanced synthesis can produce exceptionally active powders, yet commodity reactive magnesia must be manufactured continuously, consistently and safely at high solids throughput. Conversely, established kilns can process large tonnages, but long thermal exposure can promote crystal growth and eliminate the very defect and pore structure that enhances hydration or dissolution. A critical review must therefore evaluate reactivity together with conversion, energy, carbon, cost, operability and technology readiness (An et al., 2021; An et al., 2025; Cheng et al., 2024; Cheng et al., 2026; Karmil et al., 2025; Ma et al., 2023; Margaritis et al., 2023; Senevirathna et al., 2025; Telesca et al., 2024; Xu et al., 2023; Zhao et al., 2022; Zhou et al., 2026).

1.4. Scope, questions, and contribution

The review addresses six questions: (i) which magnesium-bearing feedstocks can technically supply reactive MgO; (ii) which production routes provide genuine control over reactivity rather than only high laboratory activity; (iii) which operating variables dominate process–structure–reactivity relationships; (iv) how heterogeneous reactivity tests can be interpreted without false equivalence; (v) when increased reactivity justifies additional energy, reagents, equipment or complexity; and (vi) which routes have credible industrial scale-up pathways. The intended contribution is a decision framework in which an MgO route is judged by its ability to meet an application-specific reactivity window at minimum whole-process burden, rather than by a single maximum-performance metric.

2. REVIEW METHODOLOGY AND EVIDENCE FRAMEWORK

The manuscript is presented as a structured critical narrative review rather than as a systematic or PRISMA review. The fixed core evidence corpus contains 103 peer-reviewed and technical records published between 2020 and August 2026, including primary experimental studies, pilot-scale work, process simulation and CFD, life-cycle and exergy analyses, industrial decarbonization studies, and selected reviews. The deliberately broad scope reflects the intersection of reactive MgO production with mineral processing, thermal decomposition, brine resource recovery, cement chemistry, hydrometallurgy, carbon mineralization, and industrial energy systems. General reviews were used to map the field, whereas route-specific primary studies were used to anchor process discussions (Fontana et al., 2023; Luo et al., 2026; Nobre et al., 2020; Taheri & Larachi, 2025; Zhang, Zhao, et al., 2021). Three foundational sources published before 2020 were added only to anchor industrial terminology, calcination-history effects, and hydration testing (Aphane et al., 2009; Birchal et al., 2000; Shand, 2006); they are not included in the 103-record corpus counts or evidence-class statistics.

2.1. Databases, search logic, and temporal scope

The working corpus was assembled before manuscript drafting through topic-directed literature discovery and retained against a predefined thematic logic. The core search logic was: ("reactive MgO" OR "reactive magnesia" OR "caustic calcined magnesia"

International Journal of Current Science Research and Review
ISSN: 2581-8341
Volume 09 Issue 08 August 2026
DOI: 10.47191/ijcsrr/V9-i8-44, Impact Factor: 8.048
IJCSRR @ 2026
www.ijcsrr.org

OR "light burned magnesia") AND (production OR synthesis OR calcination OR precipitation OR brucite OR magnesite OR seawater OR brine OR residue OR carbonation). Secondary strings targeted flash calcination, fluidized beds, steam calcination, dolomite, salt-lake feedstocks, magnesium hydroxide precipitation, $MgSO_4$-derived MgO, hydration, carbonation, reactivity tests, life-cycle assessment, techno-economics, and industrial scale-up. Scopus, Web of Science, ScienceDirect, and Google Scholar were used as discovery sources during corpus assembly. However, the original database export files, duplicate-removal log, and record-by-record screening exclusions were not preserved. Accordingly, the search strings document the topical scope of the review but should not be interpreted as a retrospectively reconstructable systematic-search flow.

2.2. Inclusion, exclusion, and evidence classes

Studies were retained when they addressed at least one of four causal links: production of MgO or a calcination-ready magnesium precursor; process variables controlling MgO microstructure; analytical or application tests that reveal MgO reactivity; or environmental, economic, or scale-up consequences of a production route. Papers focused on refractory dead-burned magnesia were used only when they informed sintering or process severity, and application papers were retained only when they clarified a production–reactivity relationship. For critical synthesis, the core records were classified as: A, industrial/commercial route-specific evidence; B, pilot- or continuous-route-specific evidence; C, bench-scale process experiments; D, laboratory/materials synthesis or mechanistic experiments; and E, modeling, LCA/exergy, review, or conceptual evidence. The class indicates the type and scale of evidence supporting a claim; it is not a numerical quality score and does not imply that lower-scale studies are scientifically inferior.

2.3. Post hoc evidence coding, synthesis rules, and maturity scale

Each of the 103 core records was coded post hoc by primary route/topic, evidence class, scale or study type, and the decision dimensions directly informed by the study. The coded matrix is provided as Supplementary Table S1. The resulting distribution is A = 2, B = 6, C = 58, D = 25, and E = 12 records. Because individual papers can inform more than one decision dimension, evidence coverage by dimension is not constrained to sum to 103. Numerical values were extracted only when the source reported a clearly defined basis; incompatible tests or system boundaries were not pooled, and missing or non-comparable information is reported as NR rather than imputed.

For route comparison, evidence coverage is reported categorically rather than through an unexplained performance score. A dimension is labeled Strong when at least four route-specific records support it and the set includes pilot/industrial evidence (class A or B) together with at least two experimental records (class C or D); Moderate when at least two direct route-specific records support the dimension; Limited when only one direct record is available; and Gap when no direct evidence was identified in the coded core corpus. Industrial maturity is summarized separately through a review-specific Evidence Maturity Level (EML): EML1 = conceptual/modeling/review only; EML2 = laboratory or batch proof of concept; EML3 = integrated bench or continuous-laboratory evidence with realistic process integration; EML4 = pilot/real-feed continuous evidence; and EML5 = commercial or industrial route-specific evidence. EML is used as an evidence descriptor, not as a formal technology-readiness certification.

2.4. Limitations of the review

The review has five limitations. First, the retained corpus can be audited via Supplementary Table S1, but the original database exports and exclusion log are unavailable, so completeness cannot be claimed. Second, reactivity methods vary in medium, temperature, liquid-to-solid ratio, particle size, and endpoint, preventing a meta-analysis. Third, environmental and economic studies use diverse units, energy mixes, allocation rules, and carbonation assumptions. Fourth, route-specific cost data is limited compared to synthesis and characterization studies. Fifth, the 2020–August 2026 timeframe emphasizes recent developments and omits some historical literature; foundational sources are used contextually but excluded from evidence counts. These limits justify confidence labels and avoiding pooled rankings without common bases.

Figure 1 shows the temporal distribution of the 103 publications included in the core evidence corpus from 2020 to August 2026. The distribution highlights the recent growth of research on reactive MgO, particularly in 2025, while the 2026 count reflects only January–August coverage.

International Journal of Current Science Research and Review
ISSN: 2581-8341
Volume 09 Issue 08 August 2026
DOI: 10.47191/ijcsrr/V9-i8-44, Impact Factor: 8.048
IJCSRR @ 2026
www.ijcsrr.org

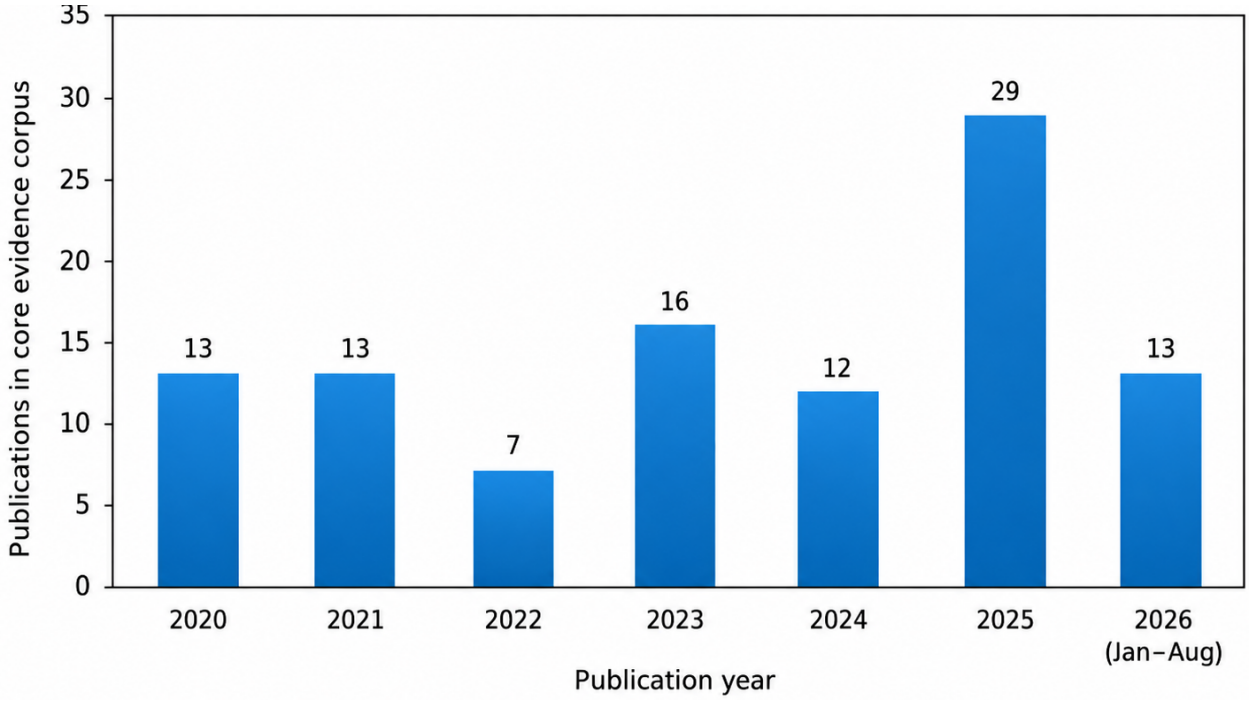

Figure 1. Temporal distribution of the 103-record core evidence corpus

Note. Author's synthesis from the 103-record core bibliography. The three pre-2020 foundational sources used for contextual anchoring are excluded. This is an evidence-corpus distribution, not a PRISMA screening count.

The year distribution shows a concentration in 2025–2026, reflecting recent interest in brine valorization, low-temperature and intensified calcination, circular MgO routes, and carbon accounting. However, recency doesn't imply maturity. The coded corpus has only 8 records in classes A–B versus 83 in C–D, indicating most evidence is experimental, not industrial. Pilot brine recovery, flash-calciner modeling, lab morphology control, and industrial magnesia decarbonization address different questions and shouldn't be weighted equally. Route comparisons in Sections 9–11 are quantitative only when based on a common report; otherwise, they use explicit coverage or maturity categories (An et al., 2025; Battaglia et al., 2024; Cheng et al., 2026; Karmil et al., 2025; Margaritis et al., 2023; Morgante et al., 2022; Senevirathna et al., 2025; Ventimiglia et al., 2025; Xu et al., 2023).

Table 1 establishes the terminology used throughout the review. The intent is to separate market labels from the underlying process features that actually control structure and reaction rate.

Table 1. Terminology and process-based classification of MgO

Term	Typical process meaning	Dominant structural tendency	Critical limitation
Caustic-calcined / light-burned MgO	Relatively mild calcination of magnesite or $Mg(OH)_2$	Higher defect density and accessible porosity than heavily fired MgO	Temperature label alone does not specify heating rate or residence time
Reactive MgO	Product engineered for a target rate/extent of dissolution, hydration, precipitation or carbonation	Application-dependent combination of mesoporosity, defects, crystallite size and accessible surface	No universal metric or universal threshold
Hard-burned MgO	Higher thermal severity and stronger sintering than light-burned product	Lower accessible surface, larger crystallites, slower reaction	May still be appropriate where delayed reaction is required

International Journal of Current Science Research and Review
ISSN: 2581-8341
Volume 09 Issue 08 August 2026
DOI: 10.47191/ijcsrr/V9-i8-44, Impact Factor: 8.048
IJCSRR @ 2026
www.ijcsrr.org

Dead-burned MgO	Very high thermal severity to maximize refractoriness and dimensional stability	Dense, highly sintered periclase	Generally outside r-MgO scope
Nanostructured / high-surface-area MgO	Specialty synthesis or templated/precipitated precursor with controlled morphology	Very high surface/defect density can be achieved	Often high cost, low throughput and not directly comparable with commodity r-MgO

Note. Author's synthesis based on Nobre et al. (2020), Bassioni et al. (2021), Bernard et al. (2023), and Wang et al. (2026).

3. WHAT MAKES MgO "REACTIVE"?

3.1. Structural origin of reactivity

MgO reactivity emerges from a hierarchy of structural features. At the crystal scale, defect-rich and poorly perfected periclase surfaces can contain energetically favorable sites for water adsorption, proton transfer and dissolution. At the particle scale, crystallite size, aggregation, pore-size distribution and tortuosity determine whether those sites are accessible. At the powder scale, particle-size distribution and agglomeration influence wetting and mass transfer. Thermal severity can progressively collapse this hierarchy by promoting neck growth, pore coarsening or closure and crystallite growth. The recent emphasis on mesopores and surface defects therefore refines, rather than replaces, the older association between light burning and rapid hydration (Hou et al., 2021; Huang et al., 2020; Lim et al., 2022; Salomão et al., 2020; Wang et al., 2026; Zhou et al., 2024).

Impurities add a second layer of control. Unreactive MgO fractions and accessory phases can reduce effective conversion in binder systems, while dissolved iron and deliberate dopants can alter hydroxylation and carbonation behavior. The direction of the effect is system-specific: impurities may block surface sites, form new phases, modify local pH or affect nucleation. Consequently, chemical purity should be reported together with phase purity, not treated as an independent scalar descriptor (Camacho Meneses et al., 2026; Li et al., 2020; Weber et al., 2025).

3.2. Reactivity is not a single metric

The literature uses BET surface area, hydration conversion, heat evolution, pH-time response, citric-acid neutralization, thermogravimetric conversion, dissolution rate, precipitation performance and CO_2 uptake as proxies for reactivity. Each interrogates a different part of the reaction sequence. BET quantifies accessible surface to nitrogen under specified conditions, but not the chemical quality of surface sites. Hydration rate integrates dissolution, transport and brucite nucleation. Acid neutralization emphasizes dissolution under an imposed chemical potential. Carbonation adds gas–liquid–solid transport and carbonate nucleation. Cobalt precipitation evaluates alkalinity release in a process solution rather than intrinsic powder behavior (Bassioni et al., 2021; Chen et al., 2026; Fedoročková et al., 2021; Gevaudan et al., 2026; Gu et al., 2026; McQueen et al., 2020; Pettauer et al., 2024; Tang et al., 2025; Wang et al., 2026).

This diversity makes direct numerical comparison hazardous. A material that hydrates rapidly can be undesirable where controlled expansion is required; a slowly dissolving MgO may be advantageous for long-duration neutralization; a high-surface powder may lose activity after humid storage; and a product optimized for CO_2 uptake may have a different pore architecture from one optimized for precipitation. The phrase 'more reactive' therefore requires a test definition, medium, temperature, liquid-to-solid ratio, particle-size condition and reaction endpoint.

Table 2 summarizes the principal analytical approaches and the property each test actually probes. A standardized reporting protocol should combine at least one structural descriptor, one direct reaction-rate test and one application-relevant endpoint.

Table 2. Analytical methods used to characterize reactive MgO

Method	Primary observable	Strength	Main caution
BET/gas adsorption	Specific surface area and pore descriptors	Sensitive to mesoporosity and accessible surface	Does not directly measure dissolution or chemical site activity
Hydration conversion / TGA	MgO → $Mg(OH)_2$ extent	Direct measure of water reaction	Depends strongly on liquid conditions and brucite-layer transport

International Journal of Current Science Research and Review
ISSN: 2581-8341
Volume 09 Issue 08 August 2026
DOI: 10.47191/ijcsrr/V9-i8-44, Impact Factor: 8.048
IJCSRR @ 2026
www.ijcsrr.org

Isothermal calorimetry	Reaction heat vs time	Kinetic fingerprint	Interpretation varies with formulation and dilution
pH-time / acid neutralization	Alkalinity release/dissolution	Simple process-relevant screening	Affected by buffering, ionic strength and particle size
XRD / crystallite analysis	Phase identity and structural order	Separates MgO from precursor or secondary phases	Bulk average may miss reactive surface fraction
CO_2 uptake/carbonation	Carbon mineralization performance	Relevant to carbon-removal and binder routes	Couples hydration, gas transfer and phase formation
Application test	Precipitation, strength, contaminant removal, etc.	Highest functional relevance	Cannot be generalized without matched conditions

Note. Author's synthesis based on Bassioni et al. (2021), Pettauer et al. (2024), Bracco et al. (2024), Weber et al. (2025), and Wang et al. (2026).

Figure 2 summarizes the process–structure–reactivity–performance framework adopted in this review. It emphasizes that reactive MgO performance emerges from the combined effects of feedstock and precursor chemistry, processing history, and resulting microstructure, and must ultimately be validated against the requirements of the intended application.

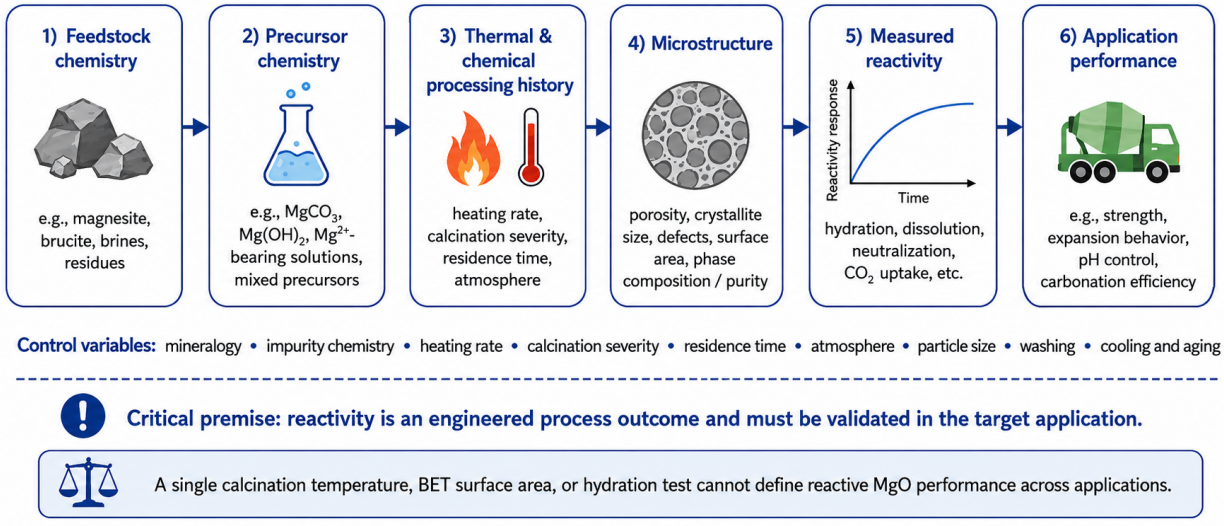

Figure 2. Process–structure–reactivity framework for reactive MgO

Note. Author's synthesis based on Huang et al. (2020), Hou et al. (2021), Salomão et al. (2020), Ababneh et al. (2025), and Wang et al. (2026).

3.3. Toward an application-specific reactivity index

A useful standard should not attempt to collapse all performance into one universal number. The proposed application-specific reactivity window is therefore organized in three mandatory reporting tiers. Tier 1 describes the material state before the reactivity test: quantitative phase composition, MgO content or purity, particle-size distribution, BET surface area and pore descriptors, and cooling/storage condition. Tier 2 describes a reproducible kinetic response under fully reported test conditions, for example a hydration conversion or rate constant, dissolution/neutralization rate, calorimetric time-to-peak, or equivalent kinetic parameter. Tier 3 is the application endpoint, such as cobalt-precipitation performance, controlled binder hydration or expansion, contaminant-removal capacity, or measured CO_2 uptake.

A reactivity window is the acceptable interval for the Tier 2 and Tier 3 responses after Tier 1 material descriptors have been matched; it is not a single universal score. For hydrometallurgical neutralization or cobalt precipitation, the window should prioritize dissolution and alkalinity-delivery kinetics together with precipitation yield and impurity control. For MgO-based cements,

International Journal of Current Science Research and Review
ISSN: 2581-8341
Volume 09 Issue 08 August 2026
DOI: 10.47191/ijcsrr/V9-i8-44, Impact Factor: 8.048
IJCSRR @ 2026
www.ijcsrr.org

hydration timing and dimensional or mechanical response are more relevant than maximum initial rate. For carbonation, accessible Mg, hydration state, gas–liquid–solid transport conditions, and verified CO_2 uptake within a defined period are required. Two production routes should therefore be ranked as functionally equivalent only when they satisfy the same Tier 3 acceptance criterion under comparable conditions; Tier 1–2 data then explain why one route achieves that endpoint with lower process burden.

For comparative tables in this review, NR denotes that a metric was not reported or cannot be compared on a common basis. This prevents BET surface area, calcination temperature, or any single acid/hydration test from being treated as a surrogate for universal reactivity.

4. FEEDSTOCKS AND PRECURSORS FOR REACTIVE MgO PRODUCTION

4.1. Magnesite and mineral-derived precursors

Magnesite remains the most direct mineral precursor because $MgCO_3$ decomposes to MgO with a simple solid–gas reaction. Its advantages are high magnesium density, established mining and calcination infrastructure, and direct compatibility with kiln or flash processes. Its central liabilities are stoichiometric CO_2 release during carbonate decomposition, gangue-derived impurities and the coupling of purity to mineral beneficiation. Decomposition kinetics and MgO morphology depend on grade, crystal texture, atmosphere and heating program, as shown for high-grade, microcrystalline and low-grade magnesites (Gong et al., 2025; Gu et al., 2026; Hou et al., 2021; Li et al., 2025; Ma et al., 2024; Smadi et al., 2023; Tang et al., 2026).

Low-grade ores and tailings broaden the resource base but make impurity management a first-class design variable. Ferroan magnesite tailings, magnesite sludge and desilication of tailings demonstrate that a reactive-MgO plant may require beneficiation, selective leaching, carbonation leaching or reprecipitation before calcination. These steps can raise purity but move the process from a simple thermal route toward a hybrid mineral-processing/hydrometallurgical flowsheet (Ismailov et al., 2020; Ivánová et al., 2026; Tang et al., 2026; Xue et al., 2025).

4.2. Brucite, dolomite, and hydromagnesite

Brucite offers a thermochemical advantage because $Mg(OH)_2$ decomposes to MgO and H_2O rather than releasing carbonate CO_2. Natural brucite is not universally available, but brucite can also be produced from brines or electrochemical routes. Calcination optimization still matters: incomplete dehydroxylation leaves precursor, whereas excessive thermal exposure destroys reactive surface. Brucite-derived MgO therefore avoids one emission mechanism but not the need to engineer the calcination window (Are et al., 2022; Lee et al., 2025; Shahbaz et al., 2022).

Dolomite and hydromagnesite occupy intermediate positions. Dolomite introduces Ca-bearing phases and therefore requires selective decomposition, separation or an application that tolerates or uses CaO; high-purity MgO from dolomite is feasible but not process-neutral. Hydromagnesite and other basic magnesium carbonates can decompose at lower apparent thermal severity and are increasingly considered as engineered intermediates, including brine-derived carbonation products (Bouchekrit et al., 2023; Hu et al., 2024; Kim et al., 2024; Qian et al., 2025; Wang et al., 2020; Yu et al., 2020; Zhang et al., 2025).

4.3. Seawater, desalination brines, and salt-lake streams

Seawater and concentrated brines decouple magnesium supply from mined carbonate. Their technical attraction is greatest where desalination or salt production already generates a concentrated stream that must be managed. The dominant route is selective $Mg(OH)_2$ precipitation followed by washing, dewatering and calcination, although carbonation to hydromagnesite, membrane crystallization, electrochemical separation and integrated salt recovery are also reported. The recurring process constraints are Mg/Ca selectivity, alkali consumption, chloride and boron removal, precursor morphology, mother-liquor management and the solids-handling behavior of fine precipitates (Ahmed, 2026; Battaglia et al., 2023; Battaglia et al., 2024; Chu et al., 2023; Dong et al., 2023; Fontana et al., 2023; Jakić, Jakić, et al., 2020; Jakić, Labor, et al., 2020; Jia et al., 2025; La Corte et al., 2020; Lalia et al., 2021; Liu, Li, Guo, et al., 2025; Morgante et al., 2022; Romano et al., 2023; Ruan et al., 2021; Vassallo, La Corte, et al., 2021; Ventimiglia et al., 2025; Zhang, Zhao, et al., 2021; Zhu et al., 2025).

A critical distinction must be made between ‘seawater-derived’ and ‘low-impact’. Seawater provides an abundant magnesium source, but environmental performance depends on the alkali source, electricity mix, degree of brine concentration already paid for by another process, washing intensity, co-product credits and whether carbonation is actually achieved within the system boundary.

International Journal of Current Science Research and Review
ISSN: 2581-8341
Volume 09 Issue 08 August 2026
DOI: 10.47191/ijcsrr/V9-i8-44, Impact Factor: 8.048
IJCSRR @ 2026
www.ijcsrr.org

LCA studies show why route-level claims must be based on explicit functional units and boundaries rather than feedstock origin alone (Badjatya et al., 2022; Senevirathna et al., 2025; Shahbaz et al., 2022; Zhang, Arrigoni, et al., 2021).

4.4. Industrial residues and specialty precursors

Industrial and hydrometallurgical streams create a circular alternative. Nickel-laterite waste solution has been converted to a nesquehonite precursor; magnesium sulfate hydrates can be converted through carbothermic routes; salt-lake magnesium slag and bischofite wastes can be used as Mg sources; and waste magnesium oxychloride cement can be recycled to MgO. These routes are attractive when they solve a waste-management problem and displace virgin feed, but their viability depends on impurity deportment, reagent recovery, gaseous products, purification and consistency of the waste stream (Liu, Wen, et al., 2025; Pereira, 2025; Pereira & Fonseca, 2025; Pereira, 2026; Souza et al., 2020; Souza et al., 2021; Xu et al., 2023; Zhong et al., 2023).

Specialty synthesis—including electrochemical preparation and PVA-assisted or morphology-controlled $Mg(OH)_2$/MgO—can create powders with highly tailored size and shape. These studies are scientifically valuable because they isolate structure–reactivity relationships, but they should not be interpreted as direct competitors to commodity magnesia without throughput, reagent and cost evidence (Amrulloh et al., 2020; Jakić et al., 2024; Masindi, 2021; Yan et al., 2025).

The feedstock landscape is summarized in Figure 3 and Table 3. The key decision is not simply where magnesium occurs, but whether the route can transform that source into a controlled precursor without creating a larger purification, reagent, or waste burden.

Figure 3 summarizes the main links between Mg-bearing feedstocks, precursor-engineering routes, and the final production of reactive MgO. It emphasizes that route selection depends not only on feedstock origin, but also on impurity control, reagent and energy demands, waste generation, and the reactivity requirements of the target application.

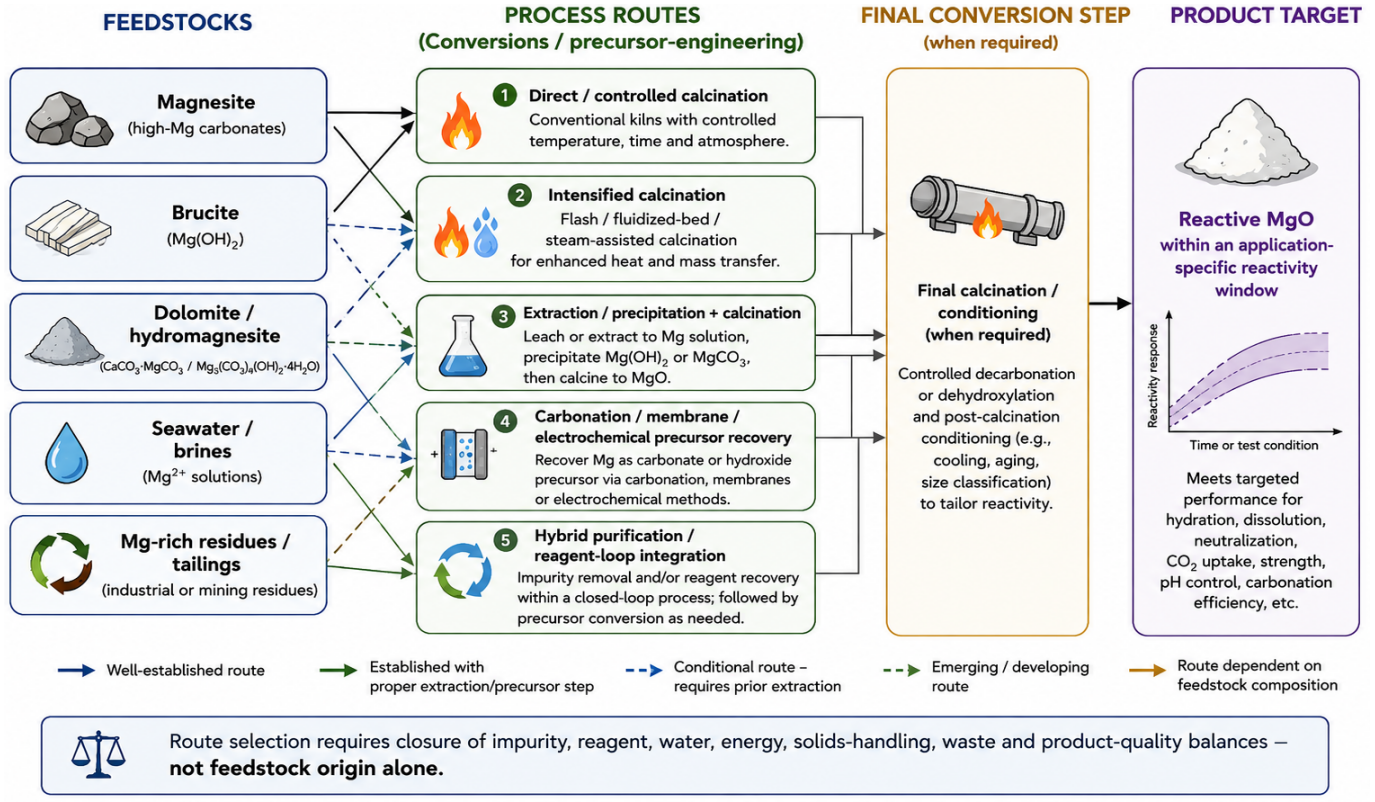

Figure 3. Feedstock-to-route map for reactive MgO production

Note. Author's synthesis based on Fontana et al. (2023), Taheri and Larachi (2025), Dong et al. (2023), Ivánová et al. (2026), and Pereira and Fonseca (2025).

International Journal of Current Science Research and Review
ISSN: 2581-8341
Volume 09 Issue 08 August 2026
DOI: 10.47191/ijcsrr/V9-i8-44, Impact Factor: 8.048
IJCSRR @ 2026
www.ijcsrr.org

Table 3. Magnesium feedstocks and precursor preparation routes

Feedstock	Typical precursor path	Main advantage	Main challenge
Magnesite	Beneficiation → $MgCO_3$ calcination	Direct and industrially mature	Process CO_2 and gangue impurities
Brucite	$Mg(OH)_2$ dehydroxylation	No carbonate-decomposition CO_2	Resource availability / precipitation burden
Dolomite	Selective calcination / leaching / precipitation	Abundant mixed carbonate source	Ca separation and product purity
Seawater / reject brine	$Mg(OH)_2$ precipitation or carbonation → calcination	Large secondary resource and circular potential	Alkali, washing, fine solids, mother liquor
Salt-lake / bischofite streams	Purification / precipitation / pyrolysis	Can valorize industrial salts and wastes	Chloride/sulfate chemistry and integration
Hydrometallurgical residues	Precipitation of Mg-carbonate/hydroxide or sulfate conversion	Waste reduction and potential reagent-loop integration	Variability and impurity deportment
Specialty synthetic precursors	Controlled precipitation / electrochemical synthesis	Morphology and purity control	Cost, throughput and scale-up

Note. Author's synthesis based on Bouchekrit et al. (2023), Dong et al. (2023), Souza et al. (2021), Xu et al. (2023), Battaglia et al. (2024), and Zhu et al. (2025).

5. THERMAL PRODUCTION ROUTES

5.1. Conventional kiln and furnace calcination

Conventional calcination remains the industrial benchmark because rotary, shaft, and related furnace technologies offer high solids throughput, robust heat supply, and established mineral handling. For reactive MgO, however, the objective differs from refractory magnesia production: decomposition must be sufficient while thermal exposure after decomposition must be minimized. The operating window is therefore bounded on one side by residual carbonate or hydroxide and on the other by sintering, crystal growth and pore loss. Studies on light-burned MgO consistently identify temperature as a major variable, but also show that product behavior depends on the full calcination history (Chen et al., 2025; Huang et al., 2020; Lim et al., 2022; Zhao et al., 2025; Zhou et al., 2024).

Industrial decarbonization options for conventional plants include alternative fuels, electrification, heat integration, and improved control. Biomass substitution and flexible-energy concepts have been analyzed for the magnesia sector, illustrating that a mature kiln route can still evolve substantially without changing the core $MgCO_3 \rightarrow MgO$ chemistry (Margaritis et al., 2022; Margaritis et al., 2023; Zhao et al., 2022).

5.2. Flash and transport-bed calcination

Flash calcination intensifies heating and shortens particle residence time. This is attractive for reactive MgO because rapid decomposition can be followed by rapid discharge before extensive sintering occurs. Transport-bed studies explicitly address energy savings, reaction characterization, and industrial justification, while CFD studies show that gas inlet design, circulation, and particle trajectories are central to scale-up. The technology therefore shifts the control problem from long kiln residence to gas–solid contacting, entrainment, residence-time distribution and thermal uniformity (An et al., 2021; An et al., 2025; Cheng et al., 2024; Cheng et al., 2026).

Elevated heating-rate experiments reinforce the mechanism: decomposition kinetics under rapid heating cannot be extrapolated directly from slow thermogravimetric conditions. This matters because reactive-MgO design increasingly targets a narrow thermal history rather than simply a target furnace temperature (Smadi et al., 2023).

5.3. Fluidized-bed, steam-assisted, solar, and emerging thermal routes

Fluidized beds can provide high gas–solid heat-transfer coefficients and more uniform particle treatment than packed or moving beds, but attrition, elutriation and gas-distribution quality become important. Numerical analysis of lightly calcined MgO

International Journal of Current Science Research and Review
ISSN: 2581-8341
Volume 09 Issue 08 August 2026
DOI: 10.47191/ijcsrr/V9-i8-44, Impact Factor: 8.048
IJCSRR @ 2026
www.ijcsrr.org

fluidized-bed roasting demonstrates the relevance of gas–solid heat transfer, while solar calcination studies indicate that renewable high-temperature heat can produce technically functional reactive-MgO cements (Ma et al., 2023; Telesca et al., 2024).

Steam calcination of magnesite is an emerging route explicitly aimed at reactive magnesia. Steam changes the reacting atmosphere and can influence heat transfer, product-gas composition, and surface chemistry. In parallel, studies of N_2 and CO_2 atmospheres show that decomposition kinetics are atmosphere-sensitive; high CO_2 partial pressure can retard carbonate decomposition or shift the required thermal history. These findings make atmosphere a genuine process variable rather than a background condition (Ababneh et al., 2025; Gong et al., 2025; Ma et al., 2024).

Electrified and solar routes are best understood as heat-supply strategies that can be combined with several reactor types. Their environmental advantage depends on electricity or solar-system boundaries, while their process advantage depends on whether they improve temperature control or simply replace the fuel. Cleaner calcination reviews for dolomite and recent gradient-calcination concepts indicate a broader move toward spatial and temporal control of thermal severity (Luo et al., 2026; Zhou et al., 2026).

Table 4 compares thermal technologies using criteria relevant to reactive MgO rather than refractory product quality.

Table 4. Comparison of thermal production technologies for reactive MgO

Route	Key control variable	Reactivity opportunity	Scale-up risk	Evidence maturity
Conventional kiln/furnace	Peak T, solids residence, gas temperature	Established control and throughput	Overburning, residence-time dispersion	EML5
Flash/transport bed	Heating rate, gas–solid contact, seconds-scale residence	Rapid conversion with limited sintering exposure	Entrained-flow control, particle separation	EML3–4
Fluidized bed	Bed hydrodynamics and heat transfer	Uniform thermal treatment	Attrition, elutriation, distributor scale-up	EML3–4
Steam-assisted calcination	Steam partial pressure and thermal history	Potential surface/kinetic modification	Steam generation and corrosion/integration	EML2–3
Solar thermal	Solar flux, reactor thermal inertia	Low-fossil process heat	Intermittency and reactor integration	EML2–3
Electrified / gradient heating	Power density and temperature zoning	Precise thermal severity control	Electricity cost, furnace throughput	EML2–3

Note. Author's synthesis based on An et al. (2025), Battaglia et al. (2024), Senevirathna et al. (2025), Telesca et al. (2024), and Zhou et al. (2026). EML definitions are given in Section 2.3.

6. CHEMICAL, HYDROCHEMICAL, AND HYBRID PRODUCTION ROUTES

6.1. Precipitation as precursor engineering

Chemical precipitation allows the MgO producer to engineer a precursor rather than accept the mineral's original morphology and impurity distribution. Mg^{2+} can be precipitated as $Mg(OH)_2$, $MgCO_3$, hydromagnesite or nesquehonite, then washed and calcined. The ability to tune supersaturation, pH, alkali addition, mixing, aging and impurity rejection is a major advantage; the countervailing burdens are reagent consumption, water use, filtration and mother-liquor treatment. Studies on NaOH precipitation, seawater bittern and Mg-rich waste streams show how precursor platelet size, purity and downstream calcination behavior are created upstream of the furnace (Battaglia et al., 2023; Battaglia et al., 2024; Jakić, Jakić, et al., 2020; Jakić, Labor, et al., 2020; Jia et al., 2025; Liu, Li, Guo, et al., 2025; Romano et al., 2023; Souza et al., 2021; Yan et al., 2025).

6.2. Membrane, electrochemical, and carbonation-assisted recovery

Membrane crystallization and electrochemical separation introduce selectivity without relying exclusively on the addition of bulk chemicals. Ion-exchange membrane crystallization has been developed from simulation through pilot-scale recovery, while selective electrochemical separation targets Ca/Mg partitioning. Carbon mineralization can simultaneously recover carbonate products and alter the pathway of magnesium precursors. These approaches are promising when energy integration or co-product

International Journal of Current Science Research and Review
ISSN: 2581-8341
Volume 09 Issue 08 August 2026
DOI: 10.47191/ijcsrr/V9-i8-44, Impact Factor: 8.048
IJCSRR @ 2026
www.ijcsrr.org

value offsets the cost of additional equipment, but they remain more complex than direct mineral calcination (La Corte et al., 2020; Lalia et al., 2021; Lu et al., 2025; Vassallo, Morgante, et al., 2021).

Carbonation-assisted routes can also convert Mg-bearing solutions to hydromagnesite, which can then be calcined at relatively low thermal severity. Seawater and concentrated brine studies demonstrate controlled carbonate precipitation, while integrated schemes may co-produce $CaCO_3$ or other salts. Their sustainability depends on CO_2 source, reagent origin, separation efficiency and whether co-products have a credible market or internal use (Kim et al., 2024; Puthanveettil et al., 2024; Zhang et al., 2023).

6.3. Waste-derived and sulfate-derived MgO

Waste-derived MgO routes are most effective when they close a process loop. $MgSO_4$ streams are important in hydrometallurgy as magnesium accumulates in sulfate circuits. Carbothermic reductive decomposition of $MgSO_4$ and hydrated $MgSO_4$ produces reactive MgO and sulfur gases, which can be used in acid regeneration. The circularity of these schemes must be balanced with reductant use, gas cleaning, sulfur recovery, and high-temperature control (Pereira, 2025; Pereira & Fonseca, 2025; Pereira, 2026; Souza et al., 2020).

Other residues require different pretreatment. Magnesite sludge has been processed through calcination, carbonation leaching and precipitation; salt-lake magnesium slag has been used as a basis for highly active MgO; bischofite waste has been analyzed by exergy and process modeling; and waste magnesium oxychloride cement can be recycled. The common lesson is that 'waste-derived' is not a process route by itself: each waste creates a specific impurity, salt and energy balance that must be closed (Ivánová et al., 2026; Liu, Wen, et al., 2025; Xu et al., 2023; Zhong et al., 2023).

6.4. Nanostructured and green synthesis routes

Electrochemical and polymer-assisted syntheses produce unusual morphologies and high surface areas, while ultrasound-assisted crystallization can influence $Mg(OH)_2$ precipitation. These methods aid in understanding nucleation and morphology control. However, a critical industrial review should treat them separately from bulk r-MgO, as laboratory activity isn't directly competitive without data on solids productivity, recycle, reagent recovery, scale, and powder handling (Amrulloh et al., 2020; Jakić, Labor, et al., 2020; Jakić et al., 2024; Masindi, 2021).

Table 5 summarizes the main hydrochemical and hybrid route families. The decisive question is whether purification and morphology control gained before calcination justify the additional separations and liquid-phase inventory.

Table 5. Chemical, brine-derived, waste-derived, and specialty production routes

Route family	Precursor/product	Primary benefit	Primary burden
Alkaline $Mg(OH)_2$ precipitation	Brucite → MgO	Purity and morphology control	Alkali, washing, fine-solids dewatering
Carbonation precipitation	Hydromagnesite/nesquehonite → MgO	Potential CO_2 use and selective precursor formation	Gas transfer, reagent balance, calcination still required
Membrane crystallization	$Mg(OH)_2$ or salts	Selective separation and process intensification	Membrane area, fouling, electrical/chemical integration
Electrochemical separation	$Mg(OH)_2$ / $CaCO_3$ co-products	Reduced bulk chemical dosing potential	Electricity and electrode/reactor scale-up
Sulfate-derived carbothermic	Reactive MgO + sulfur-bearing gas	Potential acid-loop circularity	Reductant, gas cleaning, sulfur recovery
Waste-derived hybrid	Purified Mg precursor → MgO	Waste valorization	Variable composition and multi-step purification
Nanostructured specialty	Controlled $Mg(OH)_2$/MgO morphology	High activity and tailored surface	Cost, low throughput, difficult commodity scale-up

Note. Author's synthesis based on Ruan et al. (2021), Souza et al. (2020, 2021), Chu et al. (2023), Lu et al. (2025), and Xiao et al. (2025).

International Journal of Current Science Research and Review
ISSN: 2581-8341
Volume 09 Issue 08 August 2026
DOI: 10.47191/ijcsrr/V9-i8-44, Impact Factor: 8.048
IJCSRR @ 2026
www.ijcsrr.org

7. PROCESS–STRUCTURE–REACTIVITY RELATIONSHIPS

7.1. Calcination temperature and thermal severity

Temperature is the most frequently reported process variable because it controls both precursor decomposition and sintering. At insufficient severity, residual $MgCO_3$, $Mg(OH)_2$ or intermediate carbonate phases remain. As severity increases, MgO forms, and a reactive microstructure may develop. Beyond that window, grain growth, neck formation, and pore evolution progressively reduce the number of accessible reaction sites. The optimum therefore occurs after sufficient decomposition but before unnecessary thermal densification. This trend is supported by studies of magnesite, light-burned MgO, dolomite, and calcined tailings (Birchal et al., 2000; Chen et al., 2025; Huang et al., 2020; Lim et al., 2022; Zhang et al., 2025; Zhao et al., 2025; Zhou et al., 2024).

A useful conceptual variable is 'calcination severity', which combines peak temperature, time at temperature, heating rate, and atmosphere. This avoids interpreting temperature in isolation and explains why rapid-flash or gradient processes can produce a different microstructure than a conventional furnace at a similar peak temperature.

Figure 4 illustrates the conceptual trade-off between precursor-to-MgO conversion, preservation of reactive microstructural features, and application-relevant reactivity as calcination severity increases. The optimum operating window therefore reflects a balance between sufficient conversion and retention of the structural characteristics required for the target application.

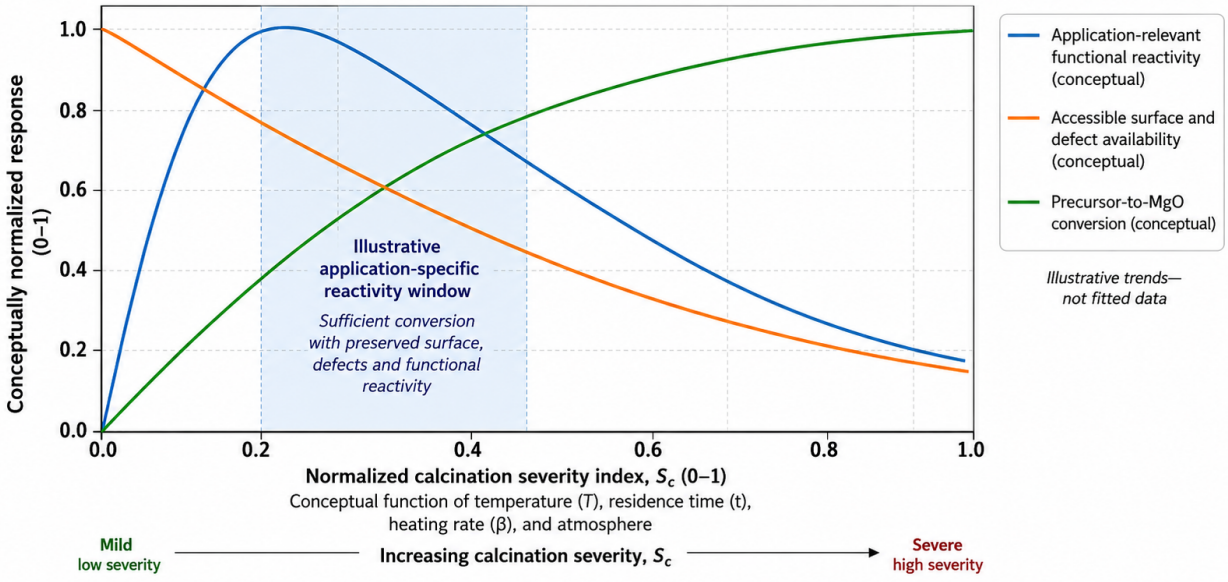

Figure 4. Conceptual relationship between calcination severity, sintering, and functional reactivity

Note. Author's conceptual synthesis based on Huang et al. (2020), Hou et al. (2021), Smadi et al. (2023), Chen et al. (2025), and Zhou et al. (2026). Curves are conceptual and are not a harmonized numerical dataset.

7.2. Residence time, heating rate, and atmosphere

Residence time determines how long newly formed MgO remains exposed to a temperature at which diffusion and sintering can proceed. This is why a short-time flash process can retain activity even when decomposition is complete, and why prolonged holding can erase the advantage of a mild peak temperature. Heating rate also changes the sequence of nucleation, pore generation, and gas evolution. Elevated-rate calcination and flash studies indicate that kinetics measured under slow laboratory heating may not reflect those in industrial intensified reactors (An et al., 2021; An et al., 2025; Hou et al., 2021; Smadi et al., 2023).

Atmosphere modifies both reaction thermodynamics and surface history. CO_2 can inhibit carbonate decomposition by raising product-gas partial pressure; N_2 provides a low-CO_2 reference environment; steam can alter transport and possibly the emerging surface; and a CO_2 self-circulation flash configuration illustrates that atmosphere can be deliberately integrated into reactor design. Consequently, kinetic models and scale-up correlations should report gas composition rather than only furnace temperature (Ababneh et al., 2025; Cheng et al., 2026; Gong et al., 2025; Ma et al., 2024).

International Journal of Current Science Research and Review
ISSN: 2581-8341
Volume 09 Issue 08 August 2026
DOI: 10.47191/ijcsrr/V9-i8-44, Impact Factor: 8.048
IJCSRR @ 2026
www.ijcsrr.org

7.3. Particle size, heat/mass transfer, and reactor hydrodynamics

Particle size influences internal heat transfer, diffusion length, gas escape, and decomposition uniformity. Fine feed reacts rapidly but increases entrainment and dust collection; coarse feed may develop radial gradients and incomplete cores. In fluidized and flash systems, particle motion and gas–solid heat transfer become coupled to cyclone or separator performance. CFD and numerical studies are therefore not merely auxiliary: they are required to translate particle-scale kinetics into reactor-scale residence-time and temperature distributions (Cheng et al., 2024; Cheng et al., 2026; Ma et al., 2023).

7.4. Impurities, precursor morphology, and post-calcination aging

Precursor morphology can persist as a structural template during decomposition. Plate-like $Mg(OH)_2$, porous hydromagnesite, and other engineered precursors can yield MgO with distinct pore architecture. Conversely, impurities can promote or inhibit local sintering, remain as inert dilution, or alter aqueous reactions. The combined influence of the alkali precursor and calcination temperature demonstrates that chemical and thermal histories cannot be cleanly separated (Jakić, Jakić, et al., 2020; Jia et al., 2025; Salomão et al., 2020; Tan et al., 2025; Wang et al., 2020).

Post-calcination exposure is an underappreciated variable. Humidity can generate reaction layers, partial hydroxylation, and changes in surface state before the material enters its intended process. Dissolved species in the eventual reaction medium can then further alter hydroxylation and carbonation. Packaging, storage time, and preconditioning should therefore be treated as part of the reactivity history, not as logistics outside the scientific problem (Bracco et al., 2024; Camacho Meneses et al., 2026; Weber et al., 2025).

Table 6 organizes the direction of these process effects. The signs are intentionally qualitative because quantitative sensitivities vary with precursor and test method.

Table 6. Influence of operating variables on MgO structure and reactivity

Variable	Increase tends to…	Potential benefit	Potential penalty
Peak temperature	Increase decomposition, then sintering	Complete precursor conversion	Loss of surface/defects if overburned
Residence time	Increase thermal exposure	Complete reaction / temperature equilibration	Crystal growth and pore loss
Heating rate	Accelerate gas release and reduce hot exposure time	Preserve transient porosity in fast processes	Thermal gradients / incomplete conversion if poorly controlled
CO_2 partial pressure	Shift carbonate decomposition conditions	Can be integrated in specialized reactors	Retards decarbonation and may raise severity requirement
Steam fraction	Modify gas transport and surface history	Potential route to tailored reactive MgO	Additional utility and corrosion/integration issues
Particle size	Increase internal transport length when coarser	Lower entrainment for coarse feed	Incomplete or nonuniform conversion
Impurity load	Change local chemistry and secondary phases	Occasional functional synergy	Dilution, passivation, uncontrolled phases
Humid aging	Pre-hydroxylate or alter surface	May be useful for deliberate conditioning	Loss of stored reactivity / inconsistent product

Note. Author's synthesis based on Huang et al. (2020), Li et al. (2020), Ma et al. (2024), Bracco et al. (2024), and Wang et al. (2026).

8. HYDRATION AND CARBONATION AS REACTIVITY VALIDATION

8.1. Hydration mechanisms and rate control

Hydration is the most broadly useful validation reaction because it directly probes the accessibility and chemical activity of MgO toward water. A simplified description is $MgO + H_2O \rightarrow Mg(OH)_2$, but the observed rate couples surface hydroxylation, Mg^{2+} dissolution, aqueous transport, brucite nucleation and growth, and eventual formation of a product layer. Depending on particle structure and solution chemistry, the controlling step can shift over time. Reviews and kinetic studies emphasize that pH,

International Journal of Current Science Research and Review
ISSN: 2581-8341
Volume 09 Issue 08 August 2026
DOI: 10.47191/ijcsrr/V9-i8-44, Impact Factor: 8.048
IJCSRR @ 2026
www.ijcsrr.org

temperature, dissolved species, and morphology all affect the apparent hydration constant (Aphane et al., 2009; Bassioni et al., 2021; Gevaudan et al., 2026; Pettauer et al., 2024; Tang et al., 2025).

For production-route comparison, hydration tests are most informative when accompanied by BET/pore analysis and phase quantification. Fast hydration can indicate a preserved defect-rich surface, but it can also be strongly altered by soluble impurities or additives. Application-specific studies in MgO-based binders demonstrate that the desired behavior may be timed rather than maximized (Bernard et al., 2023; Li et al., 2020; Lothenbach et al., 2023; Zhao et al., 2025).

8.2. Carbonation as a second validation axis

Carbonation extends the validation problem by adding CO_2 transport and carbonate precipitation. MgO may first hydrate partially, after which dissolved Mg species form carbonate-bearing phases depending on water activity, CO_2 partial pressure, temperature, and ionic composition. Ambient weathering illustrates the potential for MgO to remove CO_2 from air, whereas controlled binder and brine systems use higher CO_2 availability. Because carbonation can consume only the fraction of Mg that becomes chemically accessible, it is a useful but demanding test of pore connectivity and reaction-layer evolution (Camacho Meneses et al., 2026; Liu, Li, Yu, et al., 2025; McQueen et al., 2020; Weber et al., 2025; Zhang, Arrigoni, et al., 2021).

The sustainability implication is crucial: potential theoretical carbonation must not be automatically credited against calcination emissions. Only CO_2 uptake demonstrated within a defined life-cycle boundary should be counted. This is especially important when comparing magnesite-derived MgO, which releases stoichiometric CO_2 on calcination, with brucite- or brine-derived routes that may avoid that process emission but consume alkali or electricity.

Figure 5 shows validation pathways for the performance of reactive MgO, highlighting hydration, dissolution/neutralization, and carbonation. Their importance varies with the chemical environment and application needs.

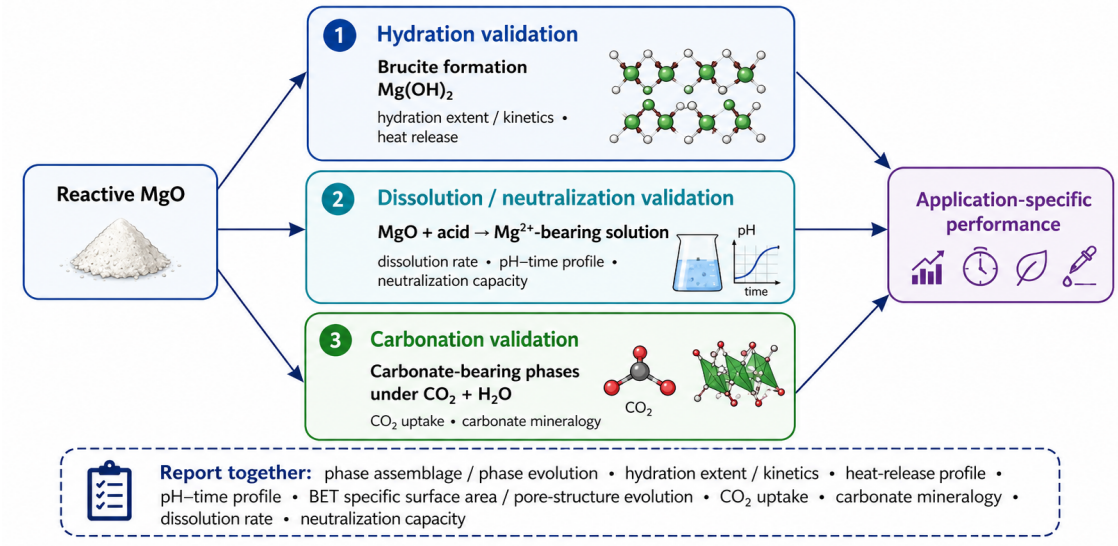

Figure 5. Hydration and carbonation as complementary validation pathways

Note. Author's synthesis based on Pettauer et al. (2024), Bracco et al. (2024), McQueen et al. (2020), Weber et al. (2025), and Camacho Meneses et al. (2026).

8.3. Application-specific reactivity

Application performance should be used as a final validation layer. In cementitious systems, a controlled hydration schedule can be more important than the fastest possible reaction. In expansive agents, delayed hydration may be intentional. In cobalt precipitation and acid neutralization, dissolution and alkalinity delivery dominate. In CO_2 mineralization, accessible Mg and carbonate-nucleation conditions are central. In sorption or permeable reactive barriers, long-term dissolution and surface accessibility may matter more than initial BET. The literature examples therefore support a matrix linking each application to a dominant reaction pathway rather than a universal activity ranking (Chen et al., 2026; Fedoročková et al., 2021; Gu et al., 2026; He et al., 2026; Lee et al., 2025; McQueen et al., 2020; Pereira, 2025).

International Journal of Current Science Research and Review
ISSN: 2581-8341
Volume 09 Issue 08 August 2026
DOI: 10.47191/ijcsrr/V9-i8-44, Impact Factor: 8.048
IJCSRR @ 2026
www.ijcsrr.org

9. COMPARATIVE ASSESSMENT OF REACTIVE MgO PRODUCTION ROUTES

A critical comparison must normalize the decision problem before ranking any route. Commodity production requires realistic feed tolerance, sufficient conversion and purity, a stable application-specific reactivity window, continuous operability, industrial solids throughput, and closed energy and waste balances. Specialty powders may rationally accept lower productivity when morphology or purity creates sufficient functional value. The comparisons below therefore separate reported quantitative benchmarks, evidence coverage, process mechanism, and evidence maturity rather than combining them in a single performance score.

Across the coded corpus, conventional magnesite calcination provides the strongest evidence of industrial-scale operability but still entails the intrinsic burden of carbonate decomposition. Flash and transport-bed routes provide stronger control of hot residence time but depend on gas–solid hydrodynamics and separation. Brucite and brine routes can avoid carbonate decomposition at the calciner and enable precursor purification, but their performance depends strongly on the upstream source of brucite, alkali demand, washing, dewatering, and mother-liquor closure. Waste-derived routes are inherently site-specific, while nanostructured routes remain principally specialty or laboratory pathways. These statements describe the type and maturity of the available evidence rather than a universal ranking of route performance.

Table 7 compiles selected quantitative benchmarks that can be stated on an explicit reported or stoichiometric basis. The values are not pooled because precursor composition, reactivity tests, energy systems, and LCA boundaries differ among studies.

Table 7. Selected quantitative benchmarks reported for reactive-MgO production routes

Route/basis	Reported condition or basis	Quantitative benchmark	Interpretive use	Source
Magnesite decarbonation	Pure $MgCO_3 \rightarrow MgO + CO_2$	1.092 kg CO_2 per kg MgO (stoichiometric)	Intrinsic process-CO_2 floor before fuel/electricity	Stoichiometric calculation
Industrial light-calcined magnesia	Chinese production inventory	1.440–2.221 kg CO_2-eq per kg product	Published cradle-to-product footprint range; boundary specific	Zhao et al. (2022)
Flash vs reverberatory calcination	Light-calcined magnesia	0.489–1.218 kg CO_2-eq/kg lower for flash calcination	Demonstrates possible equipment/process-intensification benefit	Zhao et al. (2022)
Reject-brine precipitation + calcination	NH_4OH-derived precursor; 500 °C, 2 h	BET SSA = 78.8 m^2/g	Example of high surface area obtained by precursor engineering	Dong et al. (2023)
Brine-derived MgO LCA	CaO as precipitating alkali	6.7–25.2% higher CO_2-eq than commercial MgO in the reported scenarios	Shows that avoiding mined magnesite does not guarantee lower footprint	Shahbaz et al. (2022)
Recovered brucite LCA	Reject brine; CaO precipitation	28.8–37.1% lower CO_2-eq than commercial MgO in the reported scenarios	Shows precursor/product choice and system boundary can reverse route ranking	Shahbaz et al. (2022)
Solar fluidized-bed calcination	Magnesite calcination at 850 °C	Reactive MgO suitable for the tested cement system	Demonstrates fossil-heat substitution with application validation	Telesca et al. (2024)
Sulfate-derived carbothermic route	Hydrated $MgSO_4$ route	850 °C reported as the optimum condition in the cited study	Illustrates a residue/sulfate route with a defined thermal optimum	Pereira & Fonseca (2025)

Note. Author's synthesis from the cited studies. NR values are intentionally omitted here; only benchmarks with an explicit basis are shown. The entries are not a meta-analysis and must not be interpreted as a common-basis route ranking. CO_2-eq values retain the system boundaries of the source studies.

International Journal of Current Science Research and Review
ISSN: 2581-8341
Volume 09 Issue 08 August 2026
DOI: 10.47191/ijcsrr/V9-i8-44, Impact Factor: 8.048
IJCSRR @ 2026
www.ijcsrr.org

Figure 6 summarizes the distribution and strength of evidence across the main reactive MgO production route families and key decision dimensions. The matrix highlights where the literature provides stronger support and where important gaps remain, particularly for scale-up, industrial validation, and economics.

Route family (production approach)	Decision dimensions				
	Process / reactivity	Precursor & impurity control	Energy / environmental assessment	Pilot / scale-up / industrial evidence	Economics
Conventional magnesite calcination	Moderate (n = 11)	Moderate (n = 3)	Strong (n = 8)	Limited (n = 2)	Evidence gap (n = 0)
Flash / transport-bed calcination	Strong (n = 4)	Evidence gap (n = 0)	Limited (n = 1)	Limited (n = 1)	Evidence gap (n = 0)
Brucite calcination	Moderate (n = 2)	Evidence gap (n = 0)	Evidence gap (n = 0)	Evidence gap (n = 0)	Evidence gap (n = 0)
Brine precipitation + calcination	Moderate (n = 7)	Strong (n = 11)	Moderate (n = 5)	Moderate (n = 5)	Limited (n = 1)
Waste / residue-derived hybrid routes	Strong (n = 12)	Moderate (n = 5)	Moderate (n = 2)	Limited (n = 1)	Evidence gap (n = 0)
Dolomite / hydromagnesite routes	Moderate (n = 6)	Moderate (n = 3)	Moderate (n = 2)	Evidence gap (n = 0)	Evidence gap (n = 0)
Intensified / low-carbon calcination (fluidized-bed, steam-assisted, solar/electrified)	Moderate (n = 3)	Evidence gap (n = 0)	Evidence gap (n = 0)	Evidence gap (n = 0)	Evidence gap (n = 0)
Specialty / nanoscale synthesis routes	Limited (n = 1)	Limited (n = 1)	Evidence gap (n = 0)	Evidence gap (n = 0)	Evidence gap (n = 0)

Figure 6. Evidence coverage by route family and decision dimension

Note. Author's evidence-map synthesis from Supplementary Table S1. Strong = ≥4 route-specific records including class A/B evidence plus ≥2 class C/D records; Moderate = ≥2 direct records; Limited = 1 direct record; Gap = no direct record in the coded core corpus. Cell values are evidence counts, not performance scores.

Table 8 converts the process discussion into a mechanism-focused evidence matrix. It emphasizes how each route can create reactivity, how reactivity may be lost, and the context in which the route is best supported.

Table 8. Process–structure–reactivity evidence matrix

Route	Reactivity-generating mechanism	Main loss mechanism	Best-fit context
Conventional light burning	Moderate decomposition with retained defects/porosity	Long hot residence and overburning	Large-volume established magnesia plants
Flash / transport bed	High heating rate + short post-decomposition residence	Residence-time dispersion, entrainment, incomplete coarse-particle conversion	High-throughput intensified production
Fluidized bed	Uniform heat transfer and controllable solids contacting	Attrition/elutriation and gas-distribution scale-up	Fine/controlled feed with integrated gas handling
Brucite calcination	Dehydroxylation without carbonate process CO_2	Overcalcination and upstream brucite-production burden	Natural brucite or integrated brine plants
Brine precipitation + calcination	Purity/morphology engineered before furnace	Alkali/washing/dewatering and mother liquor	Desalination or salt-industry integration
Waste-derived hybrid	Precursor purification plus waste valorization	Variable feed and multi-step chemistry	Site-specific circular process loops

International Journal of Current Science Research and Review
ISSN: 2581-8341
Volume 09 Issue 08 August 2026
DOI: 10.47191/ijcsrr/V9-i8-44, Impact Factor: 8.048
IJCSRR @ 2026
www.ijcsrr.org

Nanostructured specialty	Strong control of particle morphology and defects	Low productivity / high complexity	High-value applications

Note. Author's synthesis based on the evidence base reviewed here; representative sources include An et al. (2025), Battaglia et al. (2024), Souza et al. (2021), and Wang et al. (2026).

10. ENERGY, CARBON FOOTPRINT, AND CIRCULARITY

10.1. Energy demand and heat integration

Thermal energy is unavoidable for routes that end in calcination, but the magnitude and quality of that energy depend on precursor chemistry. Magnesite requires decarbonation; brucite requires dehydroxylation; hydromagnesite and other basic carbonates follow multi-step decomposition; precipitated precursors add upstream mixing, pumping, filtration and drying. Energy-saving therefore cannot be inferred from a lower calcination temperature alone. Drying water introduced by precipitation can offset thermal advantages if solids leave filtration at high moisture.

Process intensification offers several levers: flash heating can reduce hot residence and heat loss, fluidized beds can improve heat transfer, biomass or electrification can reduce fossil intensity, and exergy analysis can identify irreversibility in salt-derived routes. Industrial flexibility studies also show that energy-system integration may be as important as reactor chemistry (An et al., 2021; Hu et al., 2024; Ma et al., 2023; Margaritis et al., 2022; Margaritis et al., 2023; Xu et al., 2023).

10.2. Process CO_2, electricity, and upstream reagents

Carbon accounting should separate at least five contributions: stoichiometric CO_2 from carbonate decomposition; combustion emissions; electricity-related emissions; upstream reagent production; and transport/material handling. Magnesite-derived MgO has an intrinsic decarbonation term, whereas brucite-derived MgO does not. Brine-derived routes may therefore look favorable at the furnace boundary but can become reagent-intensive when NaOH, Ca-based alkalis or electrochemical separation are included. National magnesia carbon-footprint analysis, brine LCAs and route-level MgO-cement studies all demonstrate the sensitivity of conclusions to system boundaries (Senevirathna et al., 2025; Shahbaz et al., 2022; Zhang, Arrigoni, et al., 2021; Zhao et al., 2022).

A minimal common benchmark is provided by stoichiometry: decomposition of pure $MgCO_3$ releases 44.01/40.30 = 1.092 kg CO_2 per kilogram of MgO before combustion, electricity, beneficiation, and transport are counted. Published Chinese inventories place light-calcined magnesia at 1.440–2.221 kg CO_2-eq/kg product, while flash calcination was reported to reduce the footprint by 0.489–1.218 kg CO_2-eq/kg relative to reverberatory furnaces for the same product class (Zhao et al., 2022). Brine routes show why upstream chemistry must remain inside the boundary: in the scenarios of Shahbaz et al. (2022), synthetic MgO precipitated from reject brine using CaO had 6.7–25.2% higher CO_2-equivalent emissions than commercial MgO, whereas recovered brucite had 28.8–37.1% lower emissions. These values are reported examples, not transferable constants; they demonstrate that the route ranking changes with product definition, alkali source, energy mix, and system boundary.

10.3. Carbonation credit and circularity

Reactive MgO can subsequently carbonate, creating a potential climate benefit. However, credit should be granted only for measured or defensibly modeled uptake during the service life or an engineered mineralization step. Ambient weathering provides a basis for CO_2-removal concepts, while seawater-derived cement and hydromagnesite routes demonstrate more controlled mineralization opportunities. The review therefore rejects 'full theoretical carbonation' as an automatic offset to manufacturing emissions (Badjatya et al., 2022; Kim et al., 2024; Lu et al., 2025; McQueen et al., 2020; Zhang, Arrigoni, et al., 2021; Zhang et al., 2023).

Circularity is strongest when Mg recovery solves an existing residue or brine problem and when reagents or co-products circulate within the host plant. Examples include desalination brines, industrial by-product alkalis, carbide slag recycling, sulfate circuits and recycled magnesium oxychloride cement. Yet circular feed origin does not guarantee circular process performance: purges, salt accumulation, impurity buildup and low-value co-products can become new waste streams (Du et al., 2024; Pereira, 2025; Pereira, 2026; Puthanveettil et al., 2024; Xiao, Santoso, Unluer, & Yang, 2025; Xiao, Santoso, Unluer, Sun, et al., 2025; Zhong et al., 2023).

Table 9 defines an accounting framework that avoids comparing routes using inconsistent boundaries.

International Journal of Current Science Research and Review
ISSN: 2581-8341
Volume 09 Issue 08 August 2026
DOI: 10.47191/ijcsrr/V9-i8-44, Impact Factor: 8.048
IJCSRR @ 2026
www.ijcsrr.org

Table 9. Environmental, energy, and circularity indicators for route comparison

Indicator	Required boundary	Why it matters	Common misinterpretation
Calcination energy	Preheater/dryer through calciner outlet	Captures precursor-specific thermal duty	Comparing only peak temperature
Process CO_2	Direct chemical + combustion emissions	Separates unavoidable decarbonation from fuel choice	Ignoring carbonate decomposition
Electricity footprint	Pumps, membranes, electrolysis, grinding, gas handling	Critical for electrified/brine routes	Assuming electricity is zero-carbon
Reagent embodied impact	NaOH, Ca reagents, reductants, acids/bases	Can dominate indirect burden	Calling brine routes low-carbon without alkali accounting
Water/washing	Precipitation, purification, filter cake washing	Affects drying energy and effluent volume	Ignoring water carried to calcination
Verified carbonation	Measured uptake within life-cycle boundary	Potential product-stage credit	Crediting theoretical maximum uptake
Waste / co-product closure	All solids and liquid purges	Tests real circularity	Counting a by-product as a credit without market/use

Note. Author's synthesis based on Shahbaz et al. (2022), Zhao et al. (2022), Zhang, Arrigoni, et al. (2021), Senevirathna et al. (2025), and Zhou et al. (2026).

11. TECHNO-ECONOMICS, SCALABILITY, AND INDUSTRIAL READINESS

11.1. Cost drivers

The dominant cost driver changes with route family. For mined magnesite, feed beneficiation, fuel/electricity, kiln throughput, dust handling and emission control are central. For brine precipitation, alkali consumption, pumping, precipitation volume, washing, filtration and drying can dominate. For hybrid waste routes, impurity removal, reagent recycle and by-product treatment become site-specific. For intensified thermal reactors, the cost question is whether higher heat-transfer intensity and shorter residence time translate into smaller equipment or lower energy per tonne without sacrificing availability and product consistency.

Published evidence directly addressing cost remains thinner than the synthesis literature. To avoid overstating economic confidence, this review separates three evidence types. Reported cost data are numerical values or cost-effectiveness results explicitly calculated by the cited source. Process-derived cost drivers are engineering quantities—reagent consumption, energy duty, solids throughput, membrane area, filtration load, recycle, or equipment intensity—that clearly influence cost but are not themselves a complete cost estimate. Author inference is restricted to qualitative implications drawn from those drivers and is not presented as CAPEX, OPEX, or a bankable economic result. Cost-effectiveness has been reported for brine-derived alkaline-earth oxides, while industrial magnesia studies quantify energy and carbon-reduction options; pilot and simulation studies provide engineering inputs for future capital estimates but are not equivalent to bankable plant economics (Karmil et al., 2025; Margaritis et al., 2023; Morgante et al., 2022; Vassallo, La Corte, et al., 2021; Vassallo, Morgante, et al., 2021; Xu et al., 2023).

11.2. Scale-up criteria

Scale-up should be judged using solids throughput, continuous operability, heat/mass-transfer similarity, particle-size tolerance, recycle stability, equipment fouling, product recovery, maintenance, impurity control and product consistency. Flash and fluidized-bed routes require hydrodynamic similarity and robust solids separation; brine plants require precipitation and filtration performance at large slurry volumes; membrane systems require area, fouling and cleaning strategies; and waste-derived routes require feed variability control. CFD optimization and pilot brine studies are therefore particularly valuable because they expose the variables that disappear in small batch experiments (Cheng et al., 2024; Cheng et al., 2026; Ma et al., 2023; Morgante et al., 2022; Vassallo, La Corte, et al., 2021; Ventimiglia et al., 2025).

International Journal of Current Science Research and Review
ISSN: 2581-8341
Volume 09 Issue 08 August 2026
DOI: 10.47191/ijcsrr/V9-i8-44, Impact Factor: 8.048
IJCSRR @ 2026
www.ijcsrr.org

11.3. Industrial readiness and route selection

Using the review-specific EML scale defined in Section 2.3, conventional light burning reaches EML5 because commercial route-specific operation is established. Flash/transport-bed and reactive-MgO-focused fluidized-bed pathways span approximately EML3–4: integrated process and pilot evidence exists, but long-duration route-specific product-variability data remain limited. Brucite calcination also spans EML3–4 because the calcination chemistry is established, while industrial readiness depends on whether brucite is naturally available or must be produced upstream. Brine precipitation plus calcination is EML3–4 where real-feed pilot precipitation is demonstrated, but host-plant integration and mother-liquor closure remain decisive. Waste-derived hybrids and solar/electrified/gradient concepts are generally EML2–3 within the reactive-MgO context, while nanostructured specialty routes are principally EML1–2 for commodity comparison. These maturity descriptors concern the evidence supporting the complete route, not the commercial availability of individual unit operations.

Figure 7 compares the indicative maturity of the evidence for the main families of reactive MgO production routes. The EML framework distinguishes routes supported mainly by conceptual or laboratory studies from those with pilot-scale or industrial evidence, and also shows the range of maturity within the reviewed corpus.

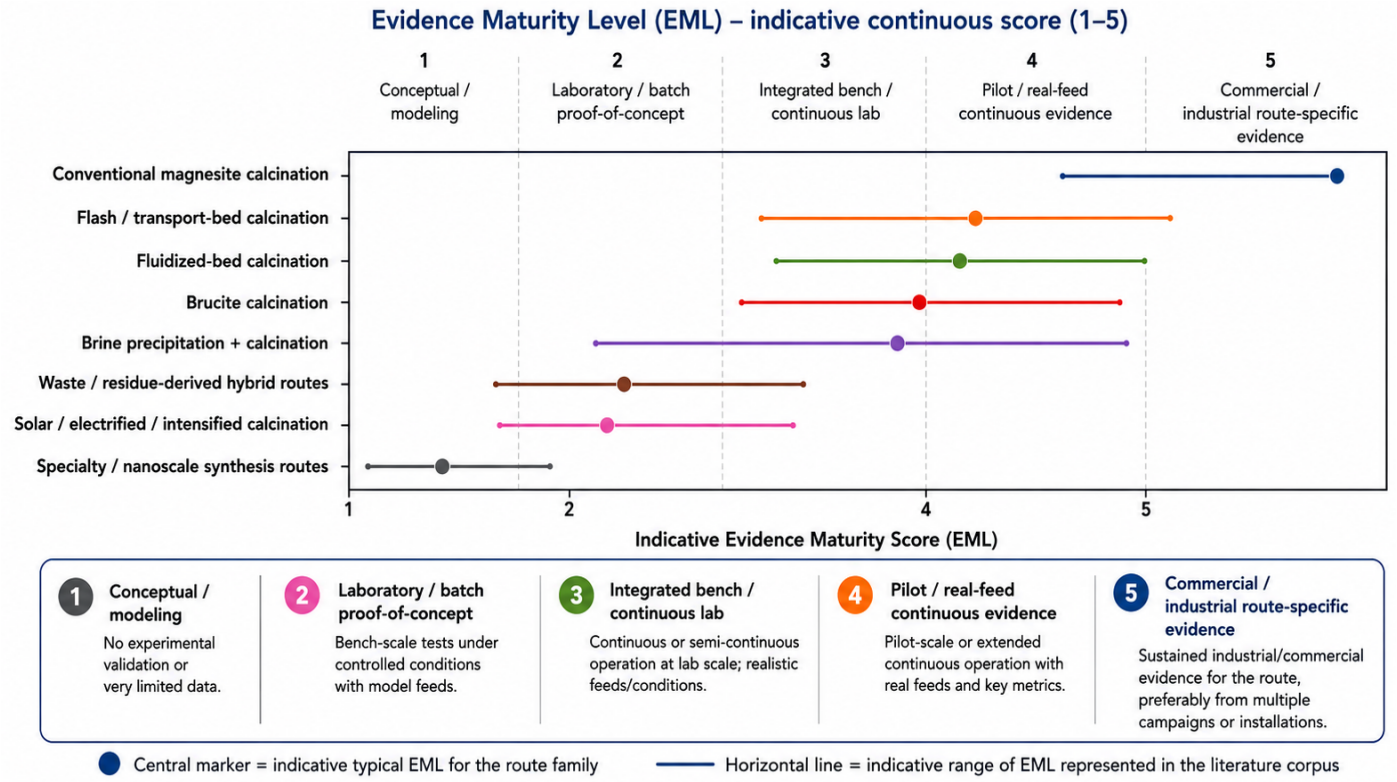

Figure 7. Indicative evidence maturity of major reactive-MgO production route families

Note. Author's synthesis using the review-specific Evidence Maturity Level (EML) defined in Section 2.3. Ranges reflect route-specific evidence in the reviewed corpus and are not formal TRL certifications or bankable cost assessments.

Table 10 links evidence maturity to the next evidence needed for decision-making. The key transition for emerging routes is from 'can make reactive MgO' to 'can make the same reactive MgO continuously, at controlled impurity and particle specifications, with a closed mass/energy/waste balance.'

International Journal of Current Science Research and Review
ISSN: 2581-8341
Volume 09 Issue 08 August 2026
DOI: 10.47191/ijcsrr/V9-i8-44, Impact Factor: 8.048
IJCSRR @ 2026
www.ijcsrr.org

Table 10. Evidence maturity, scale-up gaps, and research priorities

Route	Evidence maturity	Primary scale-up gap	Next decisive evidence
Conventional light burning	EML5	Reactivity consistency under decarbonization changes	Plant data linking thermal history to product reactivity
Flash / transport bed	EML3–4	Residence-time distribution and gas/solid separation	Long-duration continuous campaign with product variability
Fluidized bed	EML3–4	Attrition and feed-size envelope	Reactive-MgO-specific throughput and availability data
Brucite calcination	EML3–4	Brucite supply or upstream precipitation cost	Integrated plant mass-energy-cost balance
Brine precipitation + calcination	EML3–4	Alkali, washing, filtration, mother-liquor closure	Demonstration at desalination-industry scale
Waste-derived hybrid	EML2–3	Feed variability and impurity recycle	Campaign on realistic variable waste
Solar/electrified/gradient	EML2–3	Energy-system integration and availability	Continuous thermal-control demonstration plus TEA-LCA
Nanostructured specialty	EML1–2	Productivity and cost per functional unit	Market-specific TEA, not commodity comparison

Note. Author's synthesis based on An et al. (2025), Battaglia et al. (2024), Senevirathna et al. (2025), Telesca et al. (2024), and Zhou et al. (2026).

12. CRITICAL KNOWLEDGE GAPS AND RESEARCH AGENDA

12.1. A universal definition of reactive MgO is neither available nor desirable

The first gap is conceptual. A universal reactivity threshold would ignore the fact that MgO is used in systems with different desired rates and mechanisms. What is needed is standardized metadata plus application-specific performance windows. This would also prevent surface area, calcination temperature or a single acid test from becoming a surrogate definition.

12.2. Standardized reactivity testing and reporting

The minimum reporting set should include feedstock/precursor composition, phase analysis, particle-size distribution, complete thermal history, atmosphere, cooling/storage condition, MgO content, BET/pore descriptors and at least one kinetic reaction test. Studies using hydration, carbonation, dissolution or precipitation should report sufficient solution chemistry and hydrodynamic conditions for reproduction. The mechanistic literature on hydration and surface evolution provides a strong foundation for such a protocol (Bracco et al., 2024; Gevaudan et al., 2026; Pettauer et al., 2024; Tang et al., 2025; Wang et al., 2026; Weber et al., 2025).

12.3. Direct route-to-route comparative experiments

Very few studies compare multiple reactor routes using the same precursor, same target conversion, same particle-size basis and the same reactivity tests. Such experiments are essential to separate reactor effects from feedstock effects. A high-value program would compare conventional, flash, fluidized-bed and steam-assisted treatment of a common magnesite or $Mg(OH)_2$ precursor while measuring phase conversion, pore architecture, hydration, dissolution and application performance.

International Journal of Current Science Research and Review
ISSN: 2581-8341
Volume 09 Issue 08 August 2026
DOI: 10.47191/ijcsrr/V9-i8-44, Impact Factor: 8.048
IJCSRR @ 2026
www.ijcsrr.org

12.4. Pilot and continuous-plant evidence

Emerging routes must demonstrate continuous product consistency, not only average performance. Existing pilot studies in brine precipitation and process simulations in flash calcination are important steps, but long-duration campaigns should quantify fouling, solids recovery, recycle chemistry, start-up/shutdown behavior and the statistical distribution of reactivity (Battaglia et al., 2024; Cheng et al., 2024; Cheng et al., 2026; Morgante et al., 2022; Vassallo, La Corte, et al., 2021; Ventimiglia et al., 2025).

12.5. Impurity tolerance maps

The field lacks systematic impurity-tolerance maps linking Fe, Ca, Si, Al, alkalis, chloride, sulfate and trace elements to both thermal evolution and the selected reaction test. Current studies show that impurities and dissolved ions matter, but the effects are scattered across different applications. This gap is particularly important for low-grade ores, tailings, brines and residues (Ismailov et al., 2020; Li et al., 2020; Weber et al., 2025; Xue et al., 2025).

12.6. Integrated mass–energy–carbon–cost balances

The environmental and economic literature should move toward one shared process model per route family, with transparent feed composition, yields, water, reagents, heat, electricity, recycle and purge streams. LCA without process realism can over-credit carbonation or understate alkali production; TEA without product-quality constraints can favor a route that does not meet the required reactivity window. Existing LCA, exergy and carbon-footprint studies provide building blocks but not yet a fully harmonized comparison (Senevirathna et al., 2025; Shahbaz et al., 2022; Xu et al., 2023; Zhang, Arrigoni, et al., 2021; Zhao et al., 2022; Zhou et al., 2026).

12.7. Application-specific MgO design

The research question should shift from ‘How can MgO reactivity be maximized?’ to ‘What reactivity window is required for this application, and which process delivers it with the lowest whole-system burden?’ This reframing directly links powder science with process engineering and industrial decision-making. It also creates a rational basis for premium grades: a more complex route is justified only when the additional control produces measurable functional value.

Figure 8 presents the application-driven decision framework proposed for selecting, validating, and scaling reactive MgO production routes. The workflow emphasizes iterative, data-driven optimization so that the required reactivity window is achieved while minimizing whole-system energy demand, carbon footprint, cost, and process complexity

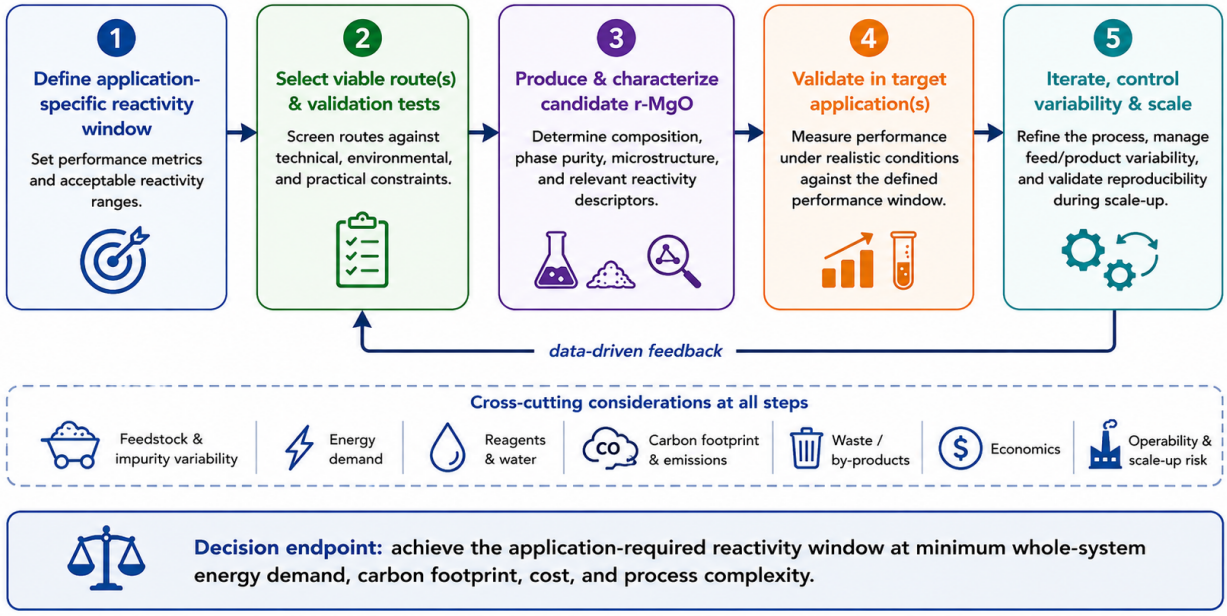

Figure 8. Research roadmap from reactivity definition to industrial decision

Note. Author’s synthesis from the critical gaps identified across the 2020–2026 core evidence corpus.

International Journal of Current Science Research and Review
ISSN: 2581-8341
Volume 09 Issue 08 August 2026
DOI: 10.47191/ijcsrr/V9-i8-44, Impact Factor: 8.048
IJCSRR @ 2026
www.ijcsrr.org

Several adjacent studies extend this agenda beyond the core route families. Struvite precipitation demonstrates that MgO by-products can have value as reactive reagents in wastewater systems; mineral recovery from rare-earth wastewater illustrates how precipitation and membrane operations can be integrated; $MgSO_4$ co-production studies show the importance of salt recovery around brine circuits; microwave-enhanced leaching of Mg-bearing tailings points to upstream intensification before MgO production; amino-acid-mediated hydration demonstrates post-production chemical conditioning; and selective leaching of calcined magnesite highlights the continuing relevance of downstream purification (Aguilar-Pozo et al., 2023; Ge et al., 2023; Kim et al., 2021; Kou et al., 2025; Puthanveettil et al., 2024; Tang et al., 2026). These studies should not be treated as direct evidence of a superior r-MgO production route, but they identify integration options and unit operations that may become important in future flowsheets.

13. CONCLUSIONS

Reactive MgO should be understood as a process-engineered material whose useful behavior is created by the combined history of feedstock, precursor chemistry, thermal or hydrochemical treatment, microstructure, impurities, and post-production exposure. This perspective explains why a temperature label, surface-area value, or single hydration test cannot define a universally superior product.

Conventional light-burned magnesite remains the most industrially mature production pathway, but its carbon burden and the risk of overburning motivate intensified and decarbonized alternatives. Flash and fluidized-bed calcination offer a technically credible route to reduce unnecessary hot residence while preserving reactive structure, provided gas–solid hydrodynamics and solids recovery are controlled. Brucite and brine-derived routes can avoid carbonate-decomposition emissions and improve purity control, but they can transfer burden to alkali production, washing, filtration, drying, electricity, and mother-liquor management. Waste-derived routes can be highly attractive when they close a site-specific process loop, although feed variability and impurity deportment constrain generalization. Specialty nanostructured routes provide the strongest morphology control but are not presently equivalent to high-volume commodity production.

The variables that most consistently determine reactivity are calcination severity, heating rate, residence time, atmosphere, precursor morphology, particle-scale heat and mass transfer, impurity chemistry, pore connectivity, mesoporosity, surface defects, and humid aging. Their importance confirms that reactivity must be measured with a combination of structural and kinetic methods and then validated in the target application.

The optimum reactive MgO is therefore not necessarily the product with the highest BET surface area, the fastest hydration, or the lowest calcination temperature. It is the product whose reaction window is matched to the intended process while meeting acceptable purity, energy demand, carbon footprint, cost, throughput, operability, and consistency. Future progress depends less on discovering another isolated high-activity powder than on standardizing reactivity definitions, comparing routes on a common basis, and demonstrating continuous production with integrated mass–energy–carbon–cost closure.

Across the coded corpus, confidence is strongest for the causal link between thermal history, microstructure, and measured reactivity and for the ability of precipitation routes to control precursor purity and morphology. Confidence is lower for direct cross-route economics, long-duration continuous product variability, and harmonized whole-system comparisons because the corresponding evidence is sparse or methodologically heterogeneous. These evidence asymmetries should guide both route selection and future experimental priorities.

DECLARATIONS

Funding: No external funding was reported for the preparation of this review.

Conflicts of Interest: The author declares no conflict of interest.

Data Availability Statement: No new experimental dataset was generated. Supplementary **Table S1** provides the post hoc coding of the 103-record core evidence corpus by primary route/topic, evidence class, study scale/type, and decision dimensions. The three foundational pre-2020 sources used only for contextual anchoring are listed in the references but are excluded from the coded core corpus.

Author Contributions: Conceptualization, methodology, critical analysis, writing—original draft, writing—review and editing: Antonio Clareti Pereira.

International Journal of Current Science Research and Review
ISSN: 2581-8341
Volume 09 Issue 08 August 2026
DOI: 10.47191/ijcsrr/V9-i8-44, Impact Factor: 8.048
IJCSRR @ 2026
www.ijcsrr.org

REFERENCES

1. Ababneh, H., Chen, A., & Dally, B. (2025). Steam calcination of magnesite for the production of reactive magnesia. Mineral Processing and Extractive Metallurgy Review, 46(8), 844–857. https://doi.org/10.1080/08827508.2024.2448788
2. Aguilar-Pozo, V.-B., Chimenos, J. M., Elduayen-Echave, B., Olaciregui-Arizmendi, K., López, A., Gómez, J., Guembe, M., García, I., Ayesa, E., & Astals, S. (2023). Struvite precipitation in wastewater treatment plants anaerobic digestion supernatants using a magnesium oxide by-product. Science of the Total Environment, 890, 164084. https://doi.org/10.1016/j.scitotenv.2023.164084
3. Ahmed, M. (2026). Experimental and process simulation study on the production of magnesium hydroxide and magnesium oxide from seawater reverse osmosis brine. Journal of Chemical and Petroleum Engineering, Article e107376. Advance online publication. https://doi.org/10.22059/jchpe.2026.408620.1695
4. Amrulloh, H., Simanjuntak, W., Situmeang, R. T. M., Sagala, S. L., Bramawanto, R., Fatiqin, A., Nahrowi, R., & Zuniati, M. (2020). Preparation of nano-magnesium oxide from Indonesia local seawater bittern using the electrochemical method. Inorganic and Nano-Metal Chemistry, 50(8), 693–698. https://doi.org/10.1080/24701556.2020.1724146
5. An, P., Han, Z., Wang, K., Cheng, J., Zhao, Z., Situmorang, Y. A., Rizkiana, J., Abudula, A., & Guan, G. (2021). Energy-saving strategy for a transport bed flash calcination process applied to magnesite. Carbon Resources Conversion, 4, 122–131. https://doi.org/10.1016/j.crcon.2021.03.004
6. An, P., Sun, Z., Song, X., Sun, C., Yan, B., Han, Z., Bai, D., & Xu, G. (2025). Flash calcination of magnesite in a one-throughput transport bed: Reaction characterization and industrial justification. Journal of Industrial and Engineering Chemistry, 143, 645–654. https://doi.org/10.1016/j.jiec.2024.09.012
7. Aphane, M. E., van der Merwe, E. M., & Strydom, C. A. (2009). Influence of hydration time on the hydration of MgO in water and in a magnesium acetate solution. Journal of Thermal Analysis and Calorimetry, 96, 987–992. https://doi.org/10.1007/s10973-008-9095-y
8. Are, C. T., Yisa, J., Suleiman, M. A. T., Auta, M., & Joseph, I. A. (2022). Optimization of the calcination of brucite for the production of magnesia using response surface methodology. Chemical Data Collections, 40, 100895. https://doi.org/10.1016/j.cdc.2022.100895
9. Badjatya, P., Akca, A. H., Fraga Alvarez, D. V., Chang, B., Ma, S., Pang, X., Wang, E., van Hinsberg, Q., Esposito, D. V., & Kawashima, S. (2022). Carbon-negative cement manufacturing from seawater-derived magnesium feedstocks. Proceedings of the National Academy of Sciences of the United States of America, 119(34), e2114680119. https://doi.org/10.1073/pnas.2114680119
10. Bassioni, G., Farid, R., Mohamed, M., Hammouda, R. M., & Kühn, F. E. (2021). Effect of different parameters on caustic magnesia hydration and magnesium hydroxide rheology: A review. Materials Advances, 2(20), 6519–6531. https://doi.org/10.1039/D0MA00887G
11. Battaglia, G., Domina, M. A., Lo Brutto, R., Lopez Rodriguez, J., Fernandez de Labastida, M., Cortina, J. L., Pettignano, A., Cipollina, A., Tamburini, A., & Micale, G. (2023). Evaluation of the purity of magnesium hydroxide recovered from saltwork bitterns. Water, 15(1), 29. https://doi.org/10.3390/w15010029
12. Battaglia, G., Ventimiglia, L., Vicari, F., Tamburini, A., Cipollina, A., & Micale, G. (2024). Characterization of $Mg(OH)_2$ powders produced from real saltworks bitterns at a pilot scale. Powder Technology, 443, 119918. https://doi.org/10.1016/j.powtec.2024.119918
13. Bernard, E., Nguyen, H., Kawashima, S., Lothenbach, B., Manzano, H., Provis, J., Scott, A., Unluer, C., Winnefeld, F., & Kinnunen, P. (2023). MgO-based cements—Current status and opportunities. RILEM Technical Letters, 8, 65–78. https://doi.org/10.21809/rilemtechlett.2023.177
14. Birchal, V. S. S., Rocha, S. D. F., & Ciminelli, V. S. T. (2000). The effect of magnesite calcination conditions on magnesia hydration. Minerals Engineering, 13(14–15), 1629–1633. https://doi.org/10.1016/S0892-6875(00)00146-1
15. Bouchekrit, C., Kolli, M., Altiner, M., & Doufnoune, R. (2023). Synthesis of high purity magnesia MgO from Algerian dolomite ore. Journal of Mining and Metallurgy, Section B: Metallurgy, 59(1), 53–64. https://doi.org/10.2298/JMMB220406005B.

International Journal of Current Science Research and Review
ISSN: 2581-8341
Volume 09 Issue 08 August 2026
DOI: 10.47191/ijcsrr/V9-i8-44, Impact Factor: 8.048
IJCSRR @ 2026
www.ijcsrr.org

16. Bracco, J. N., Camacho Meneses, G., Colón, O., Yuan, K., Stubbs, J. E., Eng, P. J., Wanhala, A. K., Einkauf, J. D., Boebinger, M. G., Stack, A. G., & Weber, J. (2024). Reaction layer formation on MgO in the presence of humidity. ACS Applied Materials & Interfaces, 16(1), 712–722. https://doi.org/10.1021/acsami.3c14823
17. Camacho Meneses, G., Yuan, K., Stack, A. G., Evans, B. R., Moseley, B., Ievlev, A. V., Borisevich, A. Y., Hernandez Penagos, P. J., Bañuelos, J. L., Chung, D. Y., Adapa, S., Einkauf, J. D., Stubbs, J. E., Eng, P. J., Boebinger, M. G., Bracco, J. N., & Weber, J. (2026). Effect of lithium doping on MgO hydroxylation and carbonation. ACS Earth and Space Chemistry, 10(3), 720–731. https://doi.org/10.1021/acsearthspacechem.5c00345
18. Chen, Y., Zhao, Y., Ngoie, M. K., Lu, X., Song, L., Weng, C., Yan, J., Sun, W., Alam, S., & Liu, W. (2026). Impact of salt-lake-based magnesia reactivity to cobalt precipitation on copper-cobalt mines, DRC. JOM, 78(5), 4336–4346. https://doi.org/10.1007/s11837-026-08137-4
19. Chen, Z., Lai, Z., Zhang, Y., Liu, Z., Lu, Z., & Li, J. (2025). Significance of low-temperature calcination in magnesite decomposition and its application in magnesium phosphate cement: A comprehensive study. Ceramics International, 51(11), 14619–14631. https://doi.org/10.1016/j.ceramint.2025.01.300
20. Cheng, D., Xu, H., Han, X., Zhao, L., Dong, H., Zhang, Z., Li, M., & Zhang, J. (2026). Optimization of operating parameters in a CO_2 self-circulation magnesite flash calciner based on CFD and NSGA-II. Chemical Engineering Research and Design, 227, 718–728. https://doi.org/10.1016/j.cherd.2026.02.018
21. Cheng, D., Xu, H., Zhao, L., Dong, H., & Zhang, Z. (2024). Effect of swirling gas inlet design on particle motion and decomposition in magnesite flash calciner. Chemical Engineering Research and Design, 206, 386–396. https://doi.org/10.1016/j.cherd.2024.04.057
22. Chu, S. H., Yang, E.-H., & Unluer, C. (2023). Chemical synthesis of magnesium oxide (MgO) from brine towards minimal energy consumption. Desalination, 556, Article 116594. https://doi.org/10.1016/j.desal.2023.116594
23. Dong, H., Xiao, X., Yang, E.-H., & Unluer, C. (2023). Recovery of ultra-high purity reactive magnesia from reject brine and its comparison with commercial magnesia. Desalination, 566, Article 116909. https://doi.org/10.1016/j.desal.2023.116909
24. Du, Z., Yang, E.-H., & Unluer, C. (2024). Investigation of the properties of $Mg(OH)_2$ extracted from magnesium-rich brine via the use of an industrial by-product. Cement and Concrete Composites, 152, Article 105658. https://doi.org/10.1016/j.cemconcomp.2024.105658
25. Fedoročková, A., Raschman, P., Sučik, G., Švandová, M., & Doráková, A. (2021). Reactive, sparingly soluble calcined magnesia, tailor-made as the reactive material for heavy metal removal from contaminated groundwater using permeable reactive barrier. Minerals, 11(11), Article 1153. https://doi.org/10.3390/min11111153
26. Fontana, D., Forte, F., Pietrantonio, M., Pucciarmati, S., & Marcoaldi, C. (2023). Magnesium recovery from seawater desalination brines: A technical review. Environment, Development and Sustainability, 25(12), 13733–13754. https://doi.org/10.1007/s10668-022-02663-2
27. Ge, X., Xie, M., Chen, G., Perera, S., Zheng, C., & Huang, M. (2023). Minerals recovery from a rare earth extraction wastewater by a combined chemical precipitation and membrane distillation process. Separation and Purification Technology, 308, Article 122899. https://doi.org/10.1016/j.seppur.2022.122899
28. Gevaudan, J. P., Ruiz-Agudo, C., Manzano, H., Nguyen, H., Lothenbach, B., Kinnunen, P., & Bernard, E. (2026). Dissolution, diffusion, and precipitation of Mg^{2+} in MgO-based cements, a review by the RILEM TC-311 MBC. Materials and Structures, 59(3), Article 161. https://doi.org/10.1617/s11527-026-03048-x
29. Gong, Z., Wang, D., Ma, X., & Fan, L. (2025). Thermal decomposition behavior and kinetics of magnesite under carbon dioxide atmosphere. Chinese Journal of Chemical Engineering, 87, 197–203. https://doi.org/10.1016/j.cjche.2025.07.014
30. Gu, X., Huang, D., Ma, Y., Ding, X., & Liu, S. (2026). Calcination behaviour, pyrolysis kinetics, and sustainable development of low-grade magnesite for high-purity MgO production. Minerals Engineering, 235, Article 109890. https://doi.org/10.1016/j.mineng.2025.109890
31. He, S., Song, X., & Tang, D. (2026). Study on the preparation and cobalt precipitation performance of highly active magnesium oxide. South African Journal of Chemical Engineering, 58, Article 100955. https://doi.org/10.1016/j.sajce.2026.100955

International Journal of Current Science Research and Review
ISSN: 2581-8341
Volume 09 Issue 08 August 2026
DOI: 10.47191/ijcsrr/V9-i8-44, Impact Factor: 8.048
IJCSRR @ 2026
www.ijcsrr.org

32. Hou, Q., Luo, X., Li, M., An, D., & Xie, Z. (2021). Non-isothermal kinetic study of high-grade magnesite thermal decomposition and morphological evolution of MgO. International Journal of Applied Ceramic Technology, 18(3), 765–772. https://doi.org/10.1111/ijac.13708.
33. Hu, C., Liu, Y., Qian, X., Qin, Y., Dong, Y., & Wang, F. (2024). Energy-saving calcination of hydromagnesite for sustainable magnesia-based cement: A new route towards MgO production. Construction and Building Materials, 419, 135593. https://doi.org/10.1016/j.conbuildmat.2024.135593
34. Huang, L., Yang, Z., & Wang, S. (2020). Influence of calcination temperature on the structure and hydration of MgO. Construction and Building Materials, 262, 120776. https://doi.org/10.1016/j.conbuildmat.2020.120776
35. Ismailov, A., Merilaita, N., Solismaa, S., Karhu, M., & Levänen, E. (2020). Utilizing mixed-mineralogy ferroan magnesite tailings as the source of magnesium oxide in magnesium potassium phosphate cement. Construction and Building Materials, 231, 117098. https://doi.org/10.1016/j.conbuildmat.2019.117098
36. Ivánová, D., Popovič, Ľ., Plešingerová, B., Sučik, G., & Raschman, P. (2026). Processing magnesite sludge into pure magnesium oxide via calcination, carbonation leaching, and precipitation. Hydrometallurgy, 244, 106803. https://doi.org/10.1016/j.hydromet.2026.106803
37. Jakić, J., Jakić, M., & Labor, M. (2020). Thermokinetic study of magnesium hydroxide obtained from seawater. Journal of Thermal Analysis and Calorimetry, 142, 2099–2110. https://doi.org/10.1007/s10973-020-10256-2
38. Jakić, J., Jakić, M., Yousefi, S., & Labor, M. (2024). PVA-assisted preparation of $Mg(OH)_2$/MgO nanostructures from seawater bittern through precipitation method. Sādhanā, 49, Article 139. https://doi.org/10.1007/s12046-024-02505-z
39. Jakić, J., Labor, M., Jozić, D., Martinac, V., & Horvat, I. (2020). Ultrasound-assisted crystallisation of magnesium hydroxide from seawater. Kemija u Industriji, 69(9–10), 473–479. https://doi.org/10.15255/KUI.2020.040
40. Jia, F., Li, Y., Guo, H., Chen, X., & Cao, J. (2025). Preparation of high-purity hexagonal flaky magnesium hydroxide and high-purity magnesium oxide from seawater bittern. Journal of Environmental Chemical Engineering, 13(5), 118008. https://doi.org/10.1016/j.jece.2025.118008
41. Karmil, F. Z., Abbassi, A., Mounkachi, O., El Alaoui-Belghiti, H., Mountadar, S., Rich, A., & Mountadar, M. (2025). Recovery of high reactive alkaline-earth-oxide (CaO and MgO) from reverse osmosis reject desalination brine: Kinetics, equilibrium, cost-effectiveness and energy-consumption. Waste Management Bulletin, 3(3), 100218. https://doi.org/10.1016/j.wmb.2025.100218
42. Kim, M.-J., Kim, S., Shin, S., & Kim, G. (2021). Production of high-purity $MgSO_4$ from seawater desalination brine. Desalination, 518, 115288. https://doi.org/10.1016/j.desal.2021.115288
43. Kim, S., Koh, E., & Kim, M.-J. (2024). Recovery of high-purity hydromagnesite from seawater through carbonation using $Ca(OH)_2$. Desalination, 586, 117907. https://doi.org/10.1016/j.desal.2024.117907
44. Kou, W., Liu, W., Liu, W., Zuo, W., & Li, W. (2025). Microwave-enhanced leaching of magnesium and iron from iron-bearing serpentine tailings. Hydrometallurgy, 237, 106536. https://doi.org/10.1016/j.hydromet.2025.106536
45. La Corte, D., Vassallo, F., Cipollina, A., Turek, M., Tamburini, A., & Micale, G. (2020). A novel ionic exchange membrane crystallizer to recover magnesium hydroxide from seawater and industrial brines. Membranes, 10(11), 303. https://doi.org/10.3390/membranes10110303
46. Lalia, B. S., Khalil, A., & Hashaikeh, R. (2021). Selective electrochemical separation and recovery of calcium and magnesium from brine. Separation and Purification Technology, 264, 118416. https://doi.org/10.1016/j.seppur.2021.118416
47. Lee, S.-H., Jeon, H. G., Davy, T., Heom, P., Hoang, A. T. P., Lee, H.-K., Lee, K.-H., & Kim, K.-W. (2025). Thermal transformation of seawater electrolysis-derived brucite into MgO: An approach for arsenic immobilization in aqueous system. Environmental Technology & Innovation, 40, 104506. https://doi.org/10.1016/j.eti.2025.104506
48. Li, S., Sun, D., Yin, Z., Wang, A., Yu, C., Wang, Y., Feng, R., & Ma, C. (2025). Thermal decomposition and non-isothermal kinetics of microcrystalline magnesite. International Journal of Applied Ceramic Technology, 22(3), e15059. https://doi.org/10.1111/ijac.15059.

International Journal of Current Science Research and Review
ISSN: 2581-8341
Volume 09 Issue 08 August 2026
DOI: 10.47191/ijcsrr/V9-i8-44, Impact Factor: 8.048
IJCSRR @ 2026
www.ijcsrr.org

49. Li, X., Qiu, R., Xue, F., & Cheng, F. (2020). Effects of unreactive MgO and impurities in light burned MgO on the hydration process and performance of base magnesium sulfate cement. Construction and Building Materials, 240, 117854. https://doi.org/10.1016/j.conbuildmat.2019.117854
50. Lim, Y.-T., So, S.-Y., & Jang, H.-S. (2022). Effect of calcination temperature on the light burned MgO matrix and its physical properties. Journal of Asian Architecture and Building Engineering, 21(2), 500–510. https://doi.org/10.1080/13467581.2020.1869021
51. Liu, S., Li, D., Yu, S., Zhang, L., Li, G., Guan, X., Zhu, J., Liu, Z., & Wang, F. (2025). Enhanced carbonation reactivity of high-magnesium low-calcium binders from magnesian limestone via low-temperature calcination. Construction and Building Materials, 489, 142414. https://doi.org/10.1016/j.conbuildmat.2025.142414
52. Liu, S., Li, Y., Guo, H., Liu, X., & Cao, J. (2025). Preparation of nano-hexagonal flake magnesium hydroxide from seawater brine and the crystallization-based separation of inorganic salt products from the mother liquor. Desalination, 612, 118954. https://doi.org/10.1016/j.desal.2025.118954
53. Liu, T., Wen, J., Zhou, L., & Tan, Y. (2025). Feasibility study on the green preparation of highly active MgO and the development of MgO-metakaolin cementitious material based on magnesium slag from Salt Lake. Construction and Building Materials, 479, 141562. https://doi.org/10.1016/j.conbuildmat.2025.141562
54. Lothenbach, B., Bernard, E., German, A., & Winnefeld, F. (2023). MgO-based binders. ce/papers, 6(6), 342–356. https://doi.org/10.1002/cepa.2774
55. Lu, P., Ochonma, P., Kim, M., Walike, C., Sunkara, A., & Gadikota, G. (2025). Electrochemical recovery of high-purity calcium carbonate and magnesium hydroxide from brine via carbon mineralization. MRS Bulletin, 50(1), 20–31. https://doi.org/10.1557/s43577-024-00804-8
56. Luo, X., Zhao, P., & Li, J. (2026). Cleaner calcination technologies of dolomite based on renewable energy: A review. Journal of Sustainable Metallurgy. Advance online publication. https://doi.org/10.1007/s40831-026-01564-2
57. Ma, X., Liu, B., Chen, G., Fan, L., & Wang, D. (2024). The kinetic mechanism of magnesite thermal decomposition under N_2 and CO_2 atmospheres. The Chinese Journal of Process Engineering, 24(8), 946–954. https://doi.org/10.12034/j.issn.1009-606X.223345
58. Ma, X.-Y., Zhao, L., Wang, D.-X., Dong, H., Liu, B., Zhang, J.-L., & Gong, Z. (2023). Numerical analysis of the gas–solid heat transfer characteristics of a lightly calcined MgO fluidized-bed roaster. Chemical Engineering Science, 267, 118334. https://doi.org/10.1016/j.ces.2022.118334
59. Margaritis, N., Evaggelou, C., Grammelis, P., Arévalo, R., Yiannoulakis, H., & Papageorgiou, P. (2023). Application of flexible tools in magnesia sector: The case of Grecian Magnesite. Sustainability, 15(16), 12130. https://doi.org/10.3390/su151612130
60. Margaritis, N., Evaggelou, C., Grammelis, P., Yiannoulakis, H., Papageorgiou, P., Puschnigg, S., & Lindorfer, J. (2022). Use of biomass as alternative fuel in magnesia sector. Fuels, 3(4), 642–666. https://doi.org/10.3390/fuels3040039
61. Masindi, V. (2021). Conversion of cryptocrystalline magnesite to MgO nanosheets: Insights into microstructural properties. Materials Today: Proceedings, 38, 1077–1087. https://doi.org/10.1016/j.matpr.2020.06.072
62. McQueen, N., Kelemen, P., Dipple, G., Renforth, P., & Wilcox, J. (2020). Ambient weathering of magnesium oxide for CO_2 removal from air. Nature Communications, 11, Article 3299. https://doi.org/10.1038/s41467-020-16510-3
63. Morgante, C., Vassallo, F., Battaglia, G., La Corte, D., Micari, M., Cipollina, A., Tamburini, A., & Micale, G. (2022). Influence of operational strategies for the recovery of magnesium hydroxide from brines at a pilot scale. Industrial & Engineering Chemistry Research, 61(41), 15355–15368. https://doi.org/10.1021/acs.iecr.2c02935
64. Nobre, J., Ahmed, H., Bravo, M., Evangelista, L., & de Brito, J. (2020). Magnesia (MgO) production and characterization, and its influence on the performance of cementitious materials: A review. Materials, 13(21), 4752. https://doi.org/10.3390/ma13214752
65. Pereira, A. C. (2025). Reactive magnesia from magnesium sulfate hydrate: A circular route for acid neutralization systems. Revista Multidisciplinar do Nordeste Mineiro, 19(3), 1–21. https://doi.org/10.61164/pma8x695

International Journal of Current Science Research and Review
ISSN: 2581-8341
Volume 09 Issue 08 August 2026
DOI: 10.47191/ijcsrr/V9-i8-44, Impact Factor: 8.048
IJCSRR @ 2026
www.ijcsrr.org

66. Pereira, A. C. (2026). Sulfuric acid regeneration from nickel laterite processing: Technologies, process chemistry, scale-up challenges, and circular economy perspectives. Journal International Review of Research Studies, 1(6), 1–58. https://doi.org/10.66104/3r2y1s96
67. Pereira, A. C., & Fonseca, R. B. da C. (2025). Synthesis of reactive MgO from hydrated magnesium sulfate via carbothermic reduction. Revista DELOS, 18(69), e6030. https://doi.org/10.55905/rdelosv18.n69-145.
68. Pettauer, M., Baldermann, A., Eder, S., & Dietzel, M. (2024). Hydration of MgO: Reaction kinetics and pH control on brucite crystal morphology. Crystal Growth & Design, 24(7), 3085–3092. https://doi.org/10.1021/acs.cgd.4c00243
69. Puthanveettil, R. K., Kim, S., & Kim, M.-J. (2024). Utilizing seawater and brine to simultaneously produce high-purity magnesium sulfate and vaterite-type calcium carbonate. Desalination, 578, 117436. https://doi.org/10.1016/j.desal.2024.117436
70. Qian, X., Qin, Y., Tao, Y., Shen, P., Hu, C., Wang, F., & Hu, S. (2025). Development of highly reactive partially calcined dolomite precursor: Synergistic effect CaO and MgO. Journal of the American Ceramic Society, 108(8), e20530. https://doi.org/10.1111/jace.20530
71. Romano, S., Trespi, S., Achermann, R., Battaglia, G., Raponi, A., Marchisio, D., Mazzotti, M., Micale, G., & Cipollina, A. (2023). The role of operating conditions in the precipitation of magnesium hydroxide hexagonal platelets using NaOH solutions. Crystal Growth & Design, 23(9), 6491–6505. https://doi.org/10.1021/acs.cgd.3c00462
72. Ruan, S., Yang, E.-H., & Unluer, C. (2021). Production of reactive magnesia from desalination reject brine and its use as a binder. Journal of CO_2 Utilization, 44, 101383. https://doi.org/10.1016/j.jcou.2020.101383
73. Salomão, R., Arruda, C. C., & Antunes, M. L. P. (2020). Synthesis, dehydroxylation and sintering of porous $Mg(OH)_2$–MgO clusters: Evolution of microstructure and physical properties. Interceram: International Ceramic Review, 69(1), 52–62. https://doi.org/10.1007/s42411-019-0067-y
74. Senevirathna, H. L., Lee, W. P. C., Wu, S., Bai, K., & Wu, P. (2025). Transforming desalination brine into highly reactive magnesium oxide and life cycle analysis. Watershed Ecology and the Environment, 7, 36–46. https://doi.org/10.1016/j.wsee.2025.01.001
75. Shahbaz, F., Singh, I., Krishnan, P., & Celik, K. (2022). Life cycle assessment of brucite and synthetic MgO produced from reject brine using different alkalis. Journal of Cleaner Production, 380, 135071. https://doi.org/10.1016/j.jclepro.2022.135071
76. Shand, M. A. (2006). The chemistry and technology of magnesia. Wiley-Interscience. https://doi.org/10.1002/0471980579
77. Smadi, E., Chinnici, A., Dally, B., & Nathan, G. J. (2023). Experimental study on the kinetics of magnesium carbonate calcination under elevated heating rates. Chemical Engineering Journal Advances, 16, 100570. https://doi.org/10.1016/j.ceja.2023.100570
78. Souza, B., Souza, R., Santos, I., & Brocchi, E. (2020). $MgSO_4$ carbothermic reductive decomposition to produce a highly reactive MgO powder. Journal of Materials Research and Technology, 9(2), 1847–1855. https://doi.org/10.1016/j.jmrt.2019.12.017
79. Souza, C. R., Vaughan, J., Rocha, S. D. F., & Birchal, V. S. (2021). Manufacturing reactive magnesia from nickel laterite waste solution via nesquehonite precipitation. Hydrometallurgy, 204, 105725. https://doi.org/10.1016/j.hydromet.2021.105725
80. Taheri, B., & Larachi, F. (2025). Mineral-based magnesium extraction technologies: Current and future practices. Processes, 13(9), 2945. https://doi.org/10.3390/pr13092945
81. Tan, S. Q., Ishak, S., Abdul Shukor Lim, N. H., Ngian, S. P., Sasui, S., & Abdullah, M. M. A. B. (2025). Physicochemical properties of reactive MgO at different alkali precursors and calcination temperatures. Journal of Environmental Chemical Engineering, 13(3), 117054. https://doi.org/10.1016/j.jece.2025.117054
82. Tang, X., Chen, S., Xu, S., Liu, H., Wang, K., Wang, Q., Zheng, C., Ji, Y., & Zhu, Y. (2026). Selective leaching optimization and kinetic mechanism of calcined magnesite in a mixed sulfuric-acetic acid system. Minerals Engineering, 237, 110003. https://doi.org/10.1016/j.mineng.2025.110003

International Journal of Current Science Research and Review
ISSN: 2581-8341
Volume 09 Issue 08 August 2026
DOI: 10.47191/ijcsrr/V9-i8-44, Impact Factor: 8.048
IJCSRR @ 2026
www.ijcsrr.org

83. Tang, X., Liu, H., Wang, K., Du, Z., Ji, Y., Zhu, Y., Meng, Q., & Liu, P. (2025). Amino acid mediated hydration of caustic calcined magnesia: Dual-function for efficient conversion and purification. Journal of Cleaner Production, 529, 146829. https://doi.org/10.1016/j.jclepro.2025.146829
84. Telesca, A., Ibris, N., Marroccoli, M., Tregambi, C., Solimene, R., Di Lauro, F., Ruiz de Ballesteros, O., Salatino, P., & Montagnaro, F. (2024). Evaluation of the technical properties of reactive-MgO cements produced by solar calcination of magnesite in a fluidized bed reactor. Renewable Energy, 225, 120231. https://doi.org/10.1016/j.renene.2024.120231.
85. Vassallo, F., La Corte, D., Cancilla, N., Tamburini, A., Bevacqua, M., Cipollina, A., & Micale, G. (2021). A pilot-plant for the selective recovery of magnesium and calcium from waste brines. Desalination, 517, 115231. https://doi.org/10.1016/j.desal.2021.115231
86. Vassallo, F., Morgante, C., Battaglia, G., La Corte, D., Micari, M., Cipollina, A., Tamburini, A., & Micale, G. (2021). A simulation tool for ion exchange membrane crystallization of magnesium hydroxide from waste brine. Chemical Engineering Research and Design, 173, 193–205. https://doi.org/10.1016/j.cherd.2021.07.008
87. Ventimiglia, L., Vassallo, F., Lo Burgio, G., Campione, A., Cammilli, L., Vicario, P., Battaglia, G., Vicari, F., Cipollina, A., Tamburini, A., & Micale, G. (2025). Pilot scale production of $Mg(OH)_2$ compounds from a real industrial reverse osmosis desalination brine. Desalination, 613, 119052. https://doi.org/10.1016/j.desal.2025.119052
88. Wang, J., Zhou, H., Song, Y., Xie, C., Unluer, C., & Ruan, S. (2026). Revisiting MgO reactivity: The critical role of mesopores and surface defects of particles. Cement and Concrete Research, 201, 108118. https://doi.org/10.1016/j.cemconres.2025.108118
89. Wang, Y., Liu, J., Shi, T., Yang, B., Li, C., Xu, H., & Yin, W. (2020). Preparation, properties and phase transition of mesoporous hydromagnesite with various morphologies from natural magnesite. Powder Technology, 364, 822–830. https://doi.org/10.1016/j.powtec.2020.01.090
90. Weber, J., Moseley, B., Yuan, K., Evans, B. R., Starchenko, V., Tajuelo Rodriguez, E., Chung, D. Y., Boebinger, M. G., McGuire, M. A., Yumnam, G., Hermann, R. P., Anovitz, L. M., & Stack, A. G. (2025). Influence of dissolved iron in solution on MgO hydroxylation and carbonation. The Journal of Physical Chemistry C, 129(1), 194–204. https://doi.org/10.1021/acs.jpcc.4c04953
91. Xiao, X., Santoso, H. S., Unluer, C., & Yang, E.-H. (2025). The use of waste concrete sludge as alkali source to recover reactive MgO from reject brine. Desalination, 600, 118470. https://doi.org/10.1016/j.desal.2024.118470
92. Xiao, X., Santoso, H. S., Unluer, C., Sun, X., & Yang, E.-H. (2025). Repeated recycling of calcium carbide slag for MgO extraction from reject brine. Desalination, 615, 119315. https://doi.org/10.1016/j.desal.2025.119315
93. Xu, H., Dong, H., Zhao, L., & Cheng, D. (2023). Exergy analysis and modeling of pilot-scale pyrolysis for magnesium oxide preparation from salt lake bischofite industrial waste. ACS Omega, 8(49), 47153–47162. https://doi.org/10.1021/acsomega.3c07165
94. Xue, Z., Feng, Y., & Li, H. (2025). Investigation on the continuous reinforcement of the reverse flotation desilication of magnesite tailings: Synergistic effect of compound collector and deep-sea microbial pretreatment. Chemical Engineering Journal, 525, 170064. https://doi.org/10.1016/j.cej.2025.170064
95. Yan, S., Guo, H., Zhang, D., Li, Y., & Cao, J. (2025). Controllable synthesis of uniform small-sized $MgCO_3$ from Mg^{2+} concentrated seawater brine for the preparation of epoxy resin composite and high purity MgO. Particuology, 97, 154–166. https://doi.org/10.1016/j.partic.2024.12.012
96. Yu, J., Qian, J., Wang, F., Qin, J., Dai, X., You, C., & Jia, X. (2020). Study of using dolomite ores as raw materials to produce magnesium phosphate cement. Construction and Building Materials, 253, 119147. https://doi.org/10.1016/j.conbuildmat.2020.119147
97. Zhang, D., Li, Y., & Cao, J. (2023). Efficient magnesium recovery from seawater desalination brine via CO_2 mineralization to synthesize hydromagnesite for uranium extraction. Desalination, 559, 116629. https://doi.org/10.1016/j.desal.2023.116629
98. Zhang, R., Arrigoni, A., & Panesar, D. K. (2021). Could reactive MgO cement be a green solution? The effect of CO_2 mineralization and manufacturing route on the potential global warming impact. Cement and Concrete Composites, 124, 104263. https://doi.org/10.1016/j.cemconcomp.2021.104263

International Journal of Current Science Research and Review
ISSN: 2581-8341
Volume 09 Issue 08 August 2026
DOI: 10.47191/ijcsrr/V9-i8-44, Impact Factor: 8.048
IJCSRR @ 2026
www.ijcsrr.org

99. Zhang, X., Zhao, W., Zhang, Y., & Jegatheesan, V. (2021). A review of resource recovery from seawater desalination brine. Reviews in Environmental Science and Bio/Technology, 20(2), 333–361. https://doi.org/10.1007/s11157-021-09570-4
100. Zhang, Y., Lai, Z., Chen, Z., Liu, Z., Lu, Z., & Li, J. (2025). Low-temperature calcination of dolomite and its application in the preparation of magnesium phosphate cement. Construction and Building Materials, 464, 140162. https://doi.org/10.1016/j.conbuildmat.2025.140162.
101. Zhao, L., Feng, J., & Dong, H. (2022). Analysis of carbon footprint and reduction approach of magnesia production in China. Journal of Cleaner Production, 334, 130194. https://doi.org/10.1016/j.jclepro.2021.130194
102. Zhao, Y., Xu, X., Sun, Z., & Gu, X. (2025). Temperature regulation for calcined magnesite tailing in basic magnesium sulfate cement: Mechanisms from hydration kinetics and products performance. Construction and Building Materials, 502, 144489. https://doi.org/10.1016/j.conbuildmat.2025.144489
103. Zhong, J., Liu, P., Mo, L., Lu, D., & Peng, S. (2023). Recycling MgO from the waste magnesium oxychloride cement (MOC): Properties, CO_2 footprint and reuse in MOC. Journal of Cleaner Production, 415, 137782. https://doi.org/10.1016/j.jclepro.2023.137782
104. Zhou, J., Guan, Y., Hu, Z., Bi, W., Chang, J., & Zhang, T. (2024). Performance variations of light burned magnesia under different calcination parameters and its effects on magnesium oxysulfate cement preparation. Construction and Building Materials, 450, 138500. https://doi.org/10.1016/j.conbuildmat.2024.138500
105. Zhou, X., Wang, M., Bai, L., Wu, C., Ma, Y., Yu, J., Dai, S., & Lai, Y. (2026). Gradient calcination strategy for controlled synthesis of low-energy and high-activity MgO: From thermal decomposition mechanism to life cycle assessment. Separation and Purification Technology, 402, 138542. https://doi.org/10.1016/j.seppur.2026.138542
106. Zhu, J., Wen, T., & Yu, J. (2025). Purification of salt lake brine by dissolution precipitation method for preparation of light-burned magnesia and sintered magnesia. Ceramics International, 51(17), 23650–23657. https://doi.org/10.1016/j.ceramint.2025.03.051.

Cite this Article: Pereira, A.C. (2026). From Magnesium Feedstocks to Reactive MgO: A Critical Review of Production Routes, Reactivity Control, Industrial Scalability, and Environmental Trade-Offs. International Journal of Current Science Research and Review, 9(8), pp. 4696-4725. DOI: https://doi.org/10.47191/ijcsrr/V9-i8-44